A Systematic Degradation Kinetics Study of Gemcitabine Hydrochloride Injection Solution

By

Sardar Mohammed Jakaria

Submitted to the graduate degree program in Pharmaceutical Chemistry and the Graduate Faculty of the University of Kansas in partial fulfillment of the requirements for the degree of Master of Science.

_____

Chairperson (Teruna J. Siahaan)

_____

Michael J. Hageman

_____

Ragheb M. AbuRmaileh

Date Defended: 29th November 2017.

The Thesis Committee for Sardar Mohammed Jakaria

certifies that this is the approved version of the following thesis:

A Systematic Degradation Kinetics Study of

Gemcitabine Hydrochloride Injection Solution

_____

Chairperson (Teruna J. Siahaan)

Date approved: 30th November 2017.

Abstract

This study was carried out to systematically evaluate the degradation kinetics of gemcitabine hydrochloride injection solution over the pH region 1–12 at 70°C. The degradation kinetics of gemcitabine were determined based on several parameters such as pH, buffer composition, temperature, ionic strength, and drug concentration. A pH-rate profile was constructed using pseudo first-order kinetic rates at 70°C after buffer effect corrections; the observed pH-rate profile was characteristically U-shaped. The degradation reactions of gemcitabine were found to be largely dependent on pH and were catalyzed by protons or hydroxyl groups at extreme pH values. Gemcitabine shows maximum stability in the pH region 7–9.5.; however, due to its solubility limitations at pH ≥ 6, the gemcitabine injection solution stability at this pH range was not determined. The gemcitabine injection solution at pH 2.5 showed a maximum stability of more than two years under the refrigerated conditions; this was derived from an Arrhenius plot. The degradation of gemcitabine in 1 N HCl at 70°C for 4 weeks did not show any anomerization. In contrast, α (0.01%) and β-uridine (~ 40%) as analogues of gemcitabine were formed upon 4 weeks incubation under thermal conditions at 70°C. In this case, the water molecules acted as both acid and base to form α- and β-uridines. A high level of anomerization to generate the α-anomer of gemcitabine and α-uridine was found in 0.1 N NaOH at 70°C for four weeks, while the β-uridine (~ 20%) was observed at lower levels in this condition. Under basic conditions, a significant degradation product was formed; using NMR spectroscopy and mass spectrometry, it was determined to be 1-(2-deoxy-2,2-difluoro-α-D-erythro-ribopyranosyl)pyrimidin-2,4(1H,3H)-dione.

Acknowledgements

My sincere appreciation goes to my parents, the late Mr. Abdul Jalil and Jahan-ara Begum for their relentless support and loving care through out my life and for making my education a success. In addition, I send my appreciation to my wife, children (Farah Ayesha, Huzaifa and Saad), brothers, and sister for their patience, loving care, and support throughout my Master's study and research. I would like to acknowledge my research advisor, Dr. Teruna Siahaan, for the opportunity to study and do research under his leadership. I will forever be grateful for his mentorship and contributions towards my scientific education and for his guidance to my academic life. I would also like to acknowledge my committee members and the entire faculty of the University of Kansas Pharmaceutical Chemistry Department for their contributions, especially Dr. Valentino J. Stella and Dr. John F. Stobaugh for their sincere teaching techniques. Special thanks to Ulapane, Kavisha Raneendri, the graduate student, who generated the NMR data for my research, and Nancy Helm for all the administrative help from KU. I would like to especially acknowledge my West-Ward Pharmaceuticals colleagues, Dr. Ragheb M. AbuRamileh and Mr. Bruce C. Pittman for their valuable advice and continuous support during my research tenure. Special thanks to my other West-Ward colleagues, Dr. Ragheb H. Al-Shakhshir, Pat O Connell, Alex Herbert, Mary Ann Whalen, Dr. Lincoln Maina, Dr. Rohit Mulik, and Brandon Swan for their constant support in and out of the lab, and to Kate Siver for all the administrative help. Finally, my appreciation goes to West-Ward Pharmaceuticals for providing me the financial support and the lab facility for this research project.

Table of Contents

A. INTRODUCTION

Gemcitabine hydrochloride is a β-nucleoside (β-isomer) chemically known as 2′-deoxy-2′, 2′-difluorocytidine monohydrochloride (Scheme 1). It is an antitumor agent that inhibits DNA synthesis [1]. Gemcitabine inhibits cellular proliferation in the synthesis phase (S-phase), and has shown activity against human leukemic cell lines and a number of solid tumor types in mice [2]. As a potential *anticancer* agent, it was originally evaluated for chemotherapy by Hertel *et al*. [3], and it is used in various carcinomas to treat non-small cell lung cancer, pancreatic cancer, bladder cancer, and breast cancer. Gemcitabine is being investigated for use in oesophageal cancer, lymphomas, and various other tumor types. There are indications that it has efficacy against pancreatic cancer in patients who have had successful tumor resections [4–8].

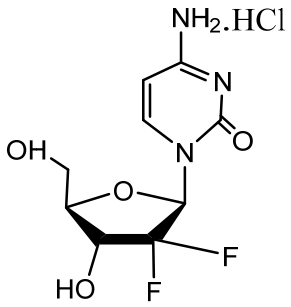

Scheme 1: Structure of gemcitabine hydrochloride . Its IUPAC name is 4-amino-1-[3,3-difluoro-4-hydroxy-5-(hydroxymethyl)-tetrahydrofuran-2-yl]-1H-pyrimidin-2-one hydrochloride. (M.W: 299.66 amu, pKa = 3.6)

The degradation of nucleosides, which undergo deamination under both acidic and basic conditions to produce the corresponding uridines, has been previously described [9]. In addition, several mechanisms for the acid-catalyzed cleavage of the N-glycosidic bond have been proposed, and anomerization of the nucleoside occurs under acidic conditions [10, 11]. Armstrong and coworkers reported the base-catalyzed anomerization of β-5-formyluridine, which involves opening of both the pyrimidine and the ribose rings to explain this unusual reaction [12].

The analysis of gemcitabine by high-performance liquid chromatography (HPLC) [13–18] and microcalorimetry [19] has been previously described. Anliker *et al.* [20] and Jansen *et al.* [21] studied the degradation of gemcitabine in solid and lyophilized forms in aqueous solution at the maximum temperatures of 40°C and 30°C, respectively. However, there has been no kinetics and mechanism degradation study of the injection solution of gemcitabine nor any identification of its degradation products.

In the present study, the degradation study of gemcitabine injection solution with identification of its degradation products was carried out to elucidate its possible degradation mechanisms. The study was carried out at pH 1–12 under the influence of various buffer compositions, ionic strengths, temperatures, and drug concentrations. The disappearance of the drug and the appearance of the degradation products were monitored by HPLC following a standard USP method [22]. Long-term solution stability was also determined at pH 2.5, and the study was designed to generate data to construct an Arrhenius plot. This plot was used to extrapolate degradation rates at temperatures lower than those used in the study. These rates can be used to estimate the shelf-life of solutions of gemcitabine at these lower temperatures. The degradation of gemcitabine in injection solution was characterized and compared in acidic and basic solutions between 40°C and 70°C. The degradation product found in basic solution at 70°C was not detectable at 40°C; this degradation product was isolated by semi-preparative HPLC and characterized by mass spectrometry and nuclear magnetic resonance (NMR) spectroscopy.

B. MATERIALS AND METHODS

B.1. Materials:

Gemcitabine hydrochloride standard was purchased from USP for formulation preparation and method analysis. Cytosine standard also was purchased from USP. All other standard compounds such as α-anomer of gemcitabine, α-uridine and β-uridine were purchased from Toronto Research Chemicals (TRC), Toronto, Ontario, Canada. HPLC-grade methanol was obtained from Burdick & Jackson, Muskegon, MI, USA. Reagent-plus grade or ACS reagent grade monobasic sodium phosphate (anhydrous), ortho-phosphoric acid, hydrochloric acid, sodium hydroxide, and LC/MS grade ammonium formate and formic acid were purchased from Fisher, Waltham, MA, USA. Milli-Q water was obtained from a Millipore water purification system (Millipore, Billerica, MA, USA).

B.2. Gemcitabine Hydrochloride Injection Solution Formulation Preparation:

The water used in the study was purged with nitrogen gas. Thereafter, the gemcitabine hydrochloride, USP standard (amount adjusted for hydrochloride salt in gemcitabine hydrochloride) was mixed with this nitrogen-purged water and mixed well until the dissolution was completed. The pH of the solution was maintained between 2 and 3, and the pH was adjusted using HCl or NaOH solution when needed. After the pH adjustment, the final bulk solution was purged again with Nitrogen. The final concentration of the drug molecule in the gemcitabine hydrochloride injection solution obtained was 38 mg/mL. The gemcitabine injection solution was stored at 2–8°C for a month prior to conducting any research activity.

B.3. Buffer Solutions:

For the kinetic studies, the following aqueous buffer solutions were used: hydrochloric acid for pH 1.7 and 2.0; phosphate (pKa_1) for pH 2.7 and 3.1; acetate for pH 4.1 and 5.3; phosphate (pKa_2) for pH 6.0, 7.0 and 8.0; carbonate (pKa_2) for pH 9.3, 10.4 and 11.0; phosphate (pKa_3) for pH 11.5; and sodium hydroxide for pH 10.9, 11.4 and 12.0. The pH values were measured at the study temperature using an Orion Ross Ultra pH electrode (ID#8102BNUMP, Thermo Scientific, Chelmsford, MA, USA) and a pH meter (Orion 3 Star, Thermo Scientific, Chelmsford, MA, USA). For a constant ionic strength (μ) of 0.3 M, each solution was adjusted with an appropriate amount of sodium chloride. This was not the case for solutions used in the experiments in which the ionic strength was varied. No significant changes in pH were observed throughout the degradation studies.

B.4. Kinetic Measurements of Drug Degradation:

The influences of various external factors on the degradation process were studied. To construct the pH-rate profile, the pH was varied between 1 and 12 at 70°C. Values for k_{obs} were calculated at constant pH, ionic strength, and temperature. Different buffer concentrations were used to determine the effect of buffer ions on the rates of degradation. The influence of ionic strength on the chemical stability of gemcitabine was investigated with 0.01 M buffer solutions at pH 2.5, 7.0, and 11.0 at 70.0 ± 0.2°C. The ionic strength was varied between 0.05 and 1.0 M by adding various amounts of sodium chloride. Degradation of gemcitabine was investigated at 42.0, 60.0, 70.0 and 80.0° ± 0.2°C in 0.01 M carbonate buffer at pH 11.0; in 0.01 M phosphate buffer at pH 7.0; and in 0.01 M hydrochloric acid at pH 2.5. The concentration of gemcitabine was varied between 198 and 1520 μg/mL in 0.01 M buffer solutions at pH 2.5, 7.0, and 11.0 with temperature of 70.0° ± 0.2°C and μ = 0.3 M. The degradation reactions were initiated by adding a 52 μL

sample of gemcitabine injection solution with an initial concentration of 38 mg/mL to 10 mL of the buffered solution to obtain an initial gemcitabine concentration of 198 μg/mL (7.5×10^{-4} M). Before adding gemcitabine, the buffer solutions were preheated to the temperature of the study. The stock solution of gemcitabine in water was kept at 4°C, and the drug was stable at this temperature for at least 4 weeks. Reaction solutions were kept in crimped capped glass vials in a thermostatically controlled water bath in the dark. All kinetics experiments were performed in duplicate [23–25].

At appropriate time intervals, 500 μL samples were withdrawn from the above reaction solutions and added to 500 μL of a precooled (4°C) 0.1 M phosphate buffer solution, pH 7. When the degradation of gemcitabine in buffer solutions of various molarities was studied, 500 μL of a 0.5 M phosphate stock solution was used to bring the reaction mixtures to 0.1 and 0.2 M buffer concentrations at a neutral pH. The final concentrations of the samples were at ~ 0.1 mg/mL. Until they were analyzed (within 2–5 days), the samples were kept at 4°C which stabilized the samples for this period of time. All samples belonging to the same experiment were analyzed on the same day by a stability indicating HPLC assay and impurity methods. UV spectra were measured for solutions that were processed in the same way as those used for HPLC analysis.

B.5. Degradation Chemistry:

Heat-degraded impurity sample solution (2 mg/mL) was prepared by transferring 1.32 mL of gemcitabine injection solution sample (38 mg/mL) into a 25 mL volumetric flask, and then placing it in an oven at 70°C for 4 weeks. After 4 weeks, the degraded sample solution was diluted to volume with milli-Q-water. The impurity sample solution was then diluted to a gemcitabine concentration of 0.1 mg/mL for assay.

Acid-degraded impurity sample solution (2 mg/mL) was prepared by transferring 1.32 mL of gemcitabine injection solution sample (38 mg/mL) in 0.5 mL of 1.0 N hydrochloric acid into a 25 mL volumetric flask, and then placing the sample in an oven at 70°C for 4 weeks. After 4 weeks, the degraded sample solution was neutralized with 1 N sodium hydroxide and diluted to volume (25 mL) with milli-Q-water. The impurity sample solution was diluted to a gemcitabine concentration of 0.1 mg/mL for assay.

Sample solution for degradation in basic conditions (2 mg/mL) was prepared by transferring 1.32 mL of gemcitabine injection solution sample (38 mg/mL) in 0.5 mL of 0.1 N sodium hydroxide into a 25 mL volumetric flask, and placing it in an oven at 70°C for 4 weeks. After 4 weeks, the degraded sample solution was neutralized with 0.1 N hydrochloric acid and diluted to volume (25 mL) with milli-Q-water. The impurity sample solution was then diluted to a gemcitabine concentration of 0.1 mg/mL for assay. 1.5 mL aliquots of all the above assay and impurity sample solutions were transferred into HPLC vials for sample injections.

B.6. Analytical HPLC:

Chromatographic separation of gemcitabine and its degradation products was performed on an Agilent HPLC system equipped with 1200 series pump, photo diode array detector, and auto sampler. For analytical HPLC, a Zorbax RX-C8 column (250 × 4.6 mm, 5 μ particle size), Agilent, Santa Clara, CA USA) was used for the separation of all known and unknown impurities from gemcitabine. The USP method that was used to separate the degradation products of gemcitabine involved mobile phase A and mobile phase B. Mobile phase A was a buffered solution that consisted of 13.8 g of anhydrous sodium phosphate monobasic and 2.5 mL of phosphoric acid in 1 L milli-Q water at pH 2.4–2.6. Mobile phase B consisted of methanol. The initial composition of mobile phase A and B was 97:3 (v/v) for 8 min. The amount of mobile phase B was then

increased to 50% over a 5-min period and was maintained at this level for 7 min prior to returning to the initial mobile phase composition over a 15-min period. Before initiating sample injections, the column was allowed to equilibrate for approximately 30 min. For both assay and impurity methods, the chromatography was performed at ambient conditions, the flow rate was 1.2 mL/min, and the sample injection volume was 20 µL. The chromatograms were obtained at 275 nm. Sample concentration was ~0.1 mg mL^{-1} prepared in buffer for kinetic measurements study.

B.7. Semi-Preparative HPLC Sample Preparation:

To isolate and identify the degradation product, 2.0 mL of 6 N sodium hydroxide solution was added to 12 mL of gemcitabine hydrochloride injection solution (concentration 38 mg/mL) in a 25 mL volumetric flask; then the mixture was placed in an 80°C oven for 5 h. After 5-h incubation, sufficient 1 N hydrochloric acid was added to neutralize the solution followed by dilution with milli-Q water to 18 mg/mL concentration of gemcitabine hydrochloride. The isolated degradation products from semi-preparative HPLC were collected using a fraction collector. The fractions from preparative chromatography containing the desired product were combined and concentrated at room temperature under high vacuum on a Buchi Rotavapor R-134 by rotary evaporation. The isolated unknown sample was analyzed for impurities using analytical HPLC; the structure of the isolated sample was then characterized using LC/MS-MS and NMR.

For semi-preparative HPLC, a X-Select C18 (150 × 10 mm, 5 µ particle size, Waters, Milford, MA USA) preparative column was used for the sample injections. The data were collected and processed using Agilent "Chemstation" 1200 series software. A linear gradient program was optimized for the separation of unknown degradation product from gemcitabine and other known degradation products where it consisted of mobile phase A and moblile phase B. The mobile phase A was a buffered solution that consisted of 10 mM ammonium formate at pH 2.75. The mobile

phase B consisted of methanol. The initial composition of mobile phase A and B was of 97:3 (v/v) for 8 min. The amount of mobile phase B was then increased to 50% over a 3-minute period and was maintained at this level for 5 min prior to returning to the initial mobile phase composition over a 10 minute period. The flow rate was set at 5 mL min^{-1}. The UV detection wavelength was at 275 nm. For each sample injection, 300 µL of the above sample concentration, 18 mg/mL (refer to Semi-Preparative HPLC Sample Preparation) was injected into the prep-HPLC system.

B.8. Mass Spectroscopy (LC-MS/MS):

The collected fraction at 0.5 mg/mL in milli-Q water was subjected to LC-MS/MS analysis to identify the degradation product. LC-MS/MS analysis was performed on LTQ Velos (Thermo Fisher Scientific, Waltham, MA, USA) coupled with an HPLC system consisting of an Agilent 1200 series low pressure quaternary degasser, auto sampler, and column oven. A Zorbax RX-C8 (250 × 4.6 mm, 5 µ particle size) HPLC column was used for the separation of all known and unknown impurities from gemcitabine. The analysis was done in a positive electrospray ionization (ESI) mode with turbo ion spray interface under the following conditions: ion source voltage IS = 3800 V; declustering potential, DP = 70 V; focusing potential, FP = 400 V; capillary temperature = 400°C; entrance potential, EP = 10 V with nitrogen gas as nebulizer at 40 psi and curtain gas as nitrogen at 25 psi.

The USP impurities method was optimized for the separation of the impurities from gemcitabine where the initial mobile phase consisted of mobile phase A (10 mM ammonium formate buffer solution, pH 2.75) and mobile phase B (methanol) in a ratio of 97:3 (v/v) for 8 min. The percentage of mobile phase B was then increased to 50% over a 5-min period. This ratio (mobile phase A and B in the ratio 50:50 (v/v)) was held for 7 min and brought back to the initial condition within 15 min. Before initiating sample injections, the column was allowed to

equilibrate for approximately 30 min. The chromatography was performed at ambient condition, and the flow rate was 0.9 mL/min. The chromatograms were obtained at 275 nm. Sample concentration was ~0.1 mg mL^{-1} prepared in milli-Q water. Mass fragmentation studies were carried out by maintaining normalized collision energy at 35 V with a range of m/z 70–500 amu.

B.9. NMR Spectroscopy:

The ^{1}H and ^{13}C NMR studies of the isolated degradation products were carried out in methanol-d4 at 25°C using 400 and 500 MHz Bruker Avance NMR spectrometers, respectively. The ^{1}H and ^{13}C chemical shifts (δ) are reported in ppm.

C. RESULTS AND DISCUSSION

The degradation kinetics of gemcitabine gemcitabine injection solution were investigated over the pH range 1–12 at 70°C. High-performance liquid chromatography (HPLC) using standard USP methods for determining assay and impurities were used for these studies. To determine the degradation kinetics of gemcitabine injection solution, the effects of pH, ionic strength, buffer concentrations, temperatures, and drug concentrations on the degradation kinetics were evaluated. Arrhenius plots were constructed to determine the effect of activation energy on the reaction mechanism at different pH levels. In addition, this plot was used to determine the long-term solution stability ($t_{95\%}$) of gemcitabine injection solution at pH 2.5. The known degradation products in thermal, acidic, and basic conditions were identified by respresentative impurity standards, and one unknown degradation product under basic conditions was isolated and identified using NMR and mass spectrometry.

C.1. Time-Dependent Degradation of Gemcitabine:

Time-dependent disappearance of GM (198 μg/mL, 7.5×10^{-4} M) and the appearance of the degradation product at pH 12 and 70°C were monitored (Figure 1 and Table 1). The amounts of

degradation products reached 60% relative to the initial amount of gemcitabine (Figure 1 and Table 1). The amount of degradation product reached 60% of the starting gemcitabine concentration after 3-h stress conditions, and the amount reached a plateau at 60% after 3 h (Figure 1 and Table 1). The mass balance that accounted for observed degradation products did not reach a total of 100% (Figure 1). This result suggests that there were additional degradation products that could not be detected using the USP standard method for impurity at a wavelength of $\lambda = 275$ nm. The disappearance of gemcitabine in this sodium hydroxide medium follows pseudo first-order kinetics (Figure 1), which is determined by linearity of the plot of the natural logarithm of residual concentrations of gemcitabine vs. time at pH 12 (Figure 1).

Table 1: Time-dependent disappearance of GM and the appearance of the degradation product measured in sodium hydroxide at pH 12 and 70°C.

Time (hr.)	(% Amount Gemcitabine)	Ln (% Amount Gemcitabine)	% Amount Degradation Product	Mass Balance (Gemcitabine remaining + Degradation Product)
0	101	4.6	0.99	102.0
1	59	4.1	37.6	96.6
2	34	3.5	53.5	87.5
3	19	2.9	60.8	79.8
4	12	2.5	61.1	73.1
5	7	1.9	62.4	69.4
6	5	1.6	61.8	66.8

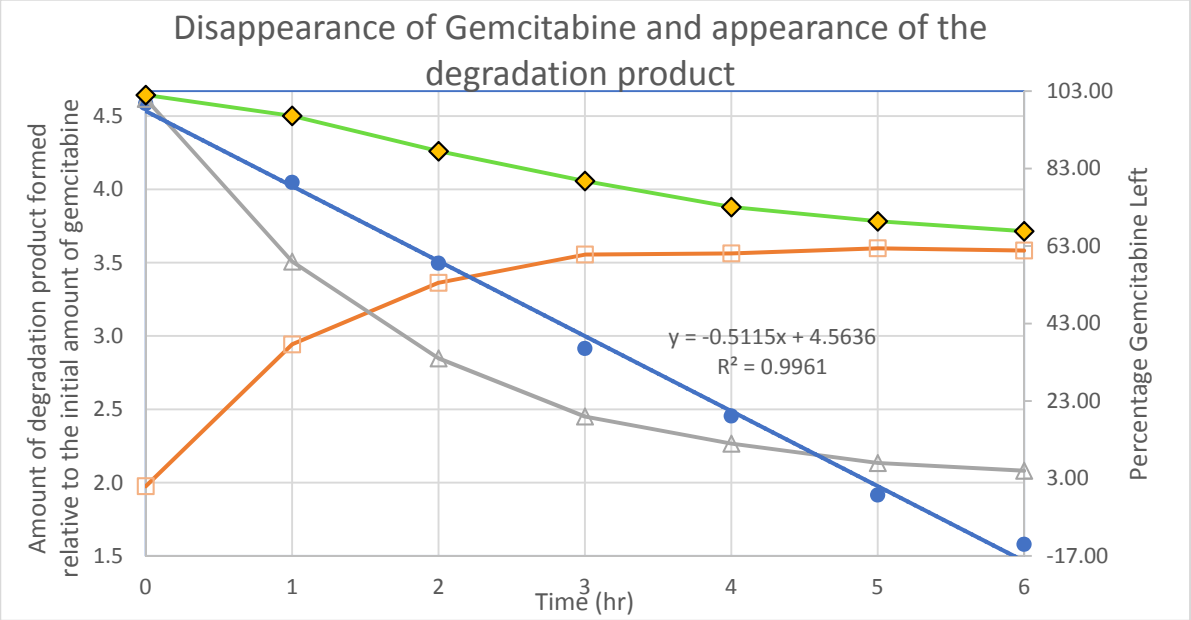

Figure 1: Time-dependent disappearance of gemcitabine and the appearance of the degradation product measured in a NaOH solution (conc. = 1 M) at pH 12 and 70°C with sample concentration = 198 µg/mL or 7.5×10^{-4} M. The Y-axis on the left represents the amount of degradation product formed relative to the initial amount of gemcitabine. The Y-axis on the right represents the amount of gemcitabine remaining. (♦ represents the mass balance of gemcitabine. Δ represents the amount of gemcitabine remaining at that time. ● represents natural logarithm of percent amount gemcitabine, which follows pseudo first-order reaction. ❑ represents the amount of degradation product formed relative to the initial amount of gemcitabine).

C.2. pH-Rate Profile of Gemcitabine at 70°C:

The pH-rate profile was constructed using the degradation rates at 70°C, µ = 0.3 M, and various pH values corrected for buffer effects (Figure 2). All rate constants obtained from individual plots of natural logarithms of sample concentration vs. time are shown in Table 2; and the specific rate constants were calculated using a non-linear least-squares curve fitting program (Table 4). The pH-rate profile shows three different regions corresponding to proton catalyzed (pH 1–6), water catalyzed (pH 7–9.5) and hydroxyl ion catalyzed (pH 10 – 12) degradation reactions, according to the following formula:

$$k_{obs} = k_0 + k_{H^+}[H^+] + k_{OH^-}[OH^-] + k_{buff}[Buffer] \qquad \text{(Eq. 1)}$$

In this case, k_0 is the rate constant of the water catalyzed reaction; k_{H^+} is the rate constant of the proton-catalyzed reaction; k_{OH^-} is the rate constant of the hydroxyl ion-catalyzed reaction. and k_{buff} **is** the rate constant of the protonated and deprotonated buffer molecule-catalyzed reactions. The degradation reactions of gemcitabine were observed as largely dependent on pH, where proton or hydroxyl catalysis occurs at extreme pH regions. Maximum stability was observed in the pH region 7.0–9.5; however, due to solubility limitations at pH ≥ 6 [26], this region was not considered for long-term stability determination. The k_{H^+} has been calculated from the straight line in the pH region 1–6 at 70°C (Table 4). The slope of –0.5 shows that something more than specific proton catalysis is likely going on (Figure 2). At the region of pH 7–9.5, K_0 was calculated where in this region log k_{obs} equals k_0 (Figure 2 and Table 4). The k_{OH^-} has been calculated from the straight line in the pH region 10–12 at 70°C (Figure 2 and Table 4). The observed slope of +1.5 indicates that something more than specific hydroxyl ion catalysis is likely going on (Figure 2).

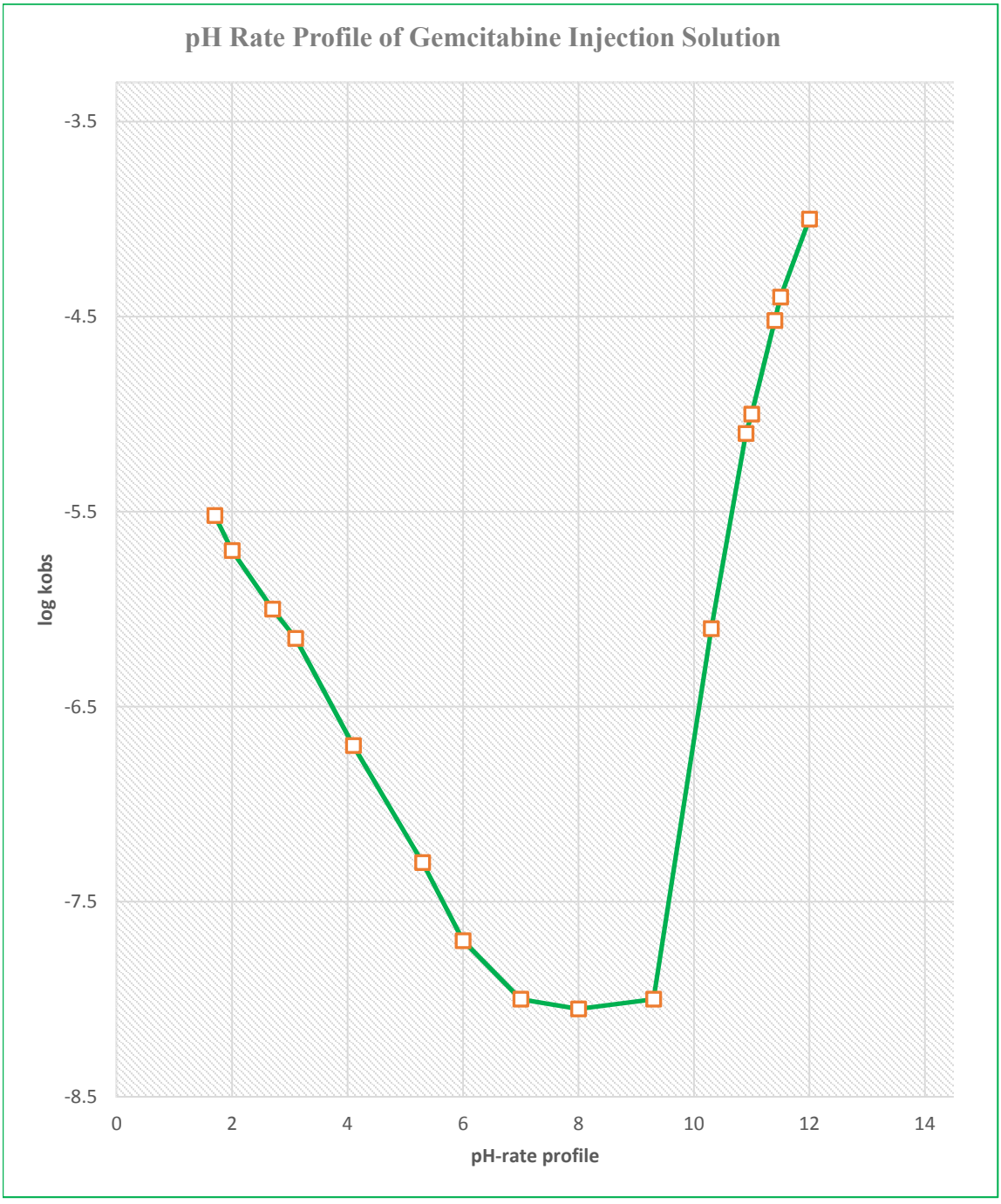

Figure 2: pH-rate profile of gemcitabine injection solution at 70°C obtained by extrapolation to zero buffer concentration. k_{H^+} = the intercept on the y-axis from the portion of the pH-rate profile between pH 1–6. (Slope = –0.5 shows something more than specific proton catalysis). From the region pH 7 – 9.5, log kobs = k_0 (no solvent effect) . k_{OH^-} = the straight line in the pH region 10 – 12 at 70°C. (Slope = +1.5 shows something more than specific hydroxyl ion catalysis). (❑ represents rate constants at each pH level).

Table 2: Summary of rate constants for degradation of gemcitabine injection solution in aqueous buffers of various pH values (70°C, μ = 0.3 M)				
Buffer Name	**Buffer Concentration (M)**	**Rate Constant k_{obs} (s^{-1}) × 10^{-5}**	**log k_{obs}**	**pH**
Sodium Hydroxide	0.10	0.8	–5.10	10.9
Sodium Hydroxide	0.25	3	–4.52	11.4
Sodium Hydroxide	1	10	–4.00	12.0
Hydrochloric Acid	0.005	0.2	–5.70	2.0
Hydrochloric Acid	0.01	0.3	–5.52	1.7
Phosphate (pKa_1)	0.01	0.1	–6.00	2.7
Phosphate (pKa_1)	0.01	0.07	–6.15	3.1
Acetate	0.01	0.02	–6.70	4.1
Acetate	0.01	0.005	–7.30	5.3
Phosphate (pKa_2)	0.01	0.002	–7.70	6.0
Phosphate (pKa_2)	0.01	0.001	–8.00	7.0
Phosphate (pKa_2)	0.01	0.0009	–8.05	8.0
Carbonate (pKa_2)	0.01	0.001	–8.00	9.3
Carbonate (pKa_2)	0.01	0.08	–6.10	10.4
Carbonate (pKa_2)	0.01	1*	–5.00	11.0
Phosphate (pKa_3)	0.01	4*	–4.40	11.5
***Influence of buffer study was conducted with various buffer concentrations (0.05 – 0.2 M), (Table 3 and Figure 3).**				

C.3. Influence of Carbonate or Phosphate Concentrations on k_{obs} for the Degradation at 70°C:

Among all buffers, carbonate and phosphate buffers were studied initially to observe significant effects on rate constant (k_{obs}) at pH region 11–11.5 (Table 3). Apparently, a proton transfer can take place as a part of the degradation mechanism in this pH region. Parallel level curves observed for both carbonate and phosphate in different buffer concentrations (0.005 M to 2.0 M) (Table 3 and Figure 3). To delete the influence of buffer ions on k_{obs}, all k_{obs} values in the pH region 11–11.5 have been extrapolated to zero buffer concentration, resulting in the corrected k'_{obs} in the pH rate profile, where the corrected k'_{obs} for carbonate buffer at pH 11.0 is 1 (y intercept = 0.7995) and for phosphate buffer at pH 11.5 is 4 (y intercept = 3.623) (Figure 3). Since the carbonate and phosphate buffers were observed with parallel level curves, for all other buffers below pH 11, the k_{obs} should have even less or no effect in various buffer concentrations between 0.05 and 0.2 M. Therefore, for all other buffers below pH 11, the buffer concentration used was 0.01 M and the final ionic strength was adjusted to 0.3 M with sodium chloride.

Table 3: Influence of carbonate and phosphate concentration on k_{obs} of the degradation reaction of gemcitabine.

Buffer Concentration (M)	**Carbonate (pKa_2) pH 11.0, k_{obs} (s^{-1}) × 10^{-5}**	**Phosphate (pKa_3) pH 11.5, k_{obs} (s^{-1}) × 10^{-5}**
0.005	1.0	4.0
0.01	0.6	3.0
0.05	1.0	4.0
0.1	0.6	4.0
0.2	1.0	4.0

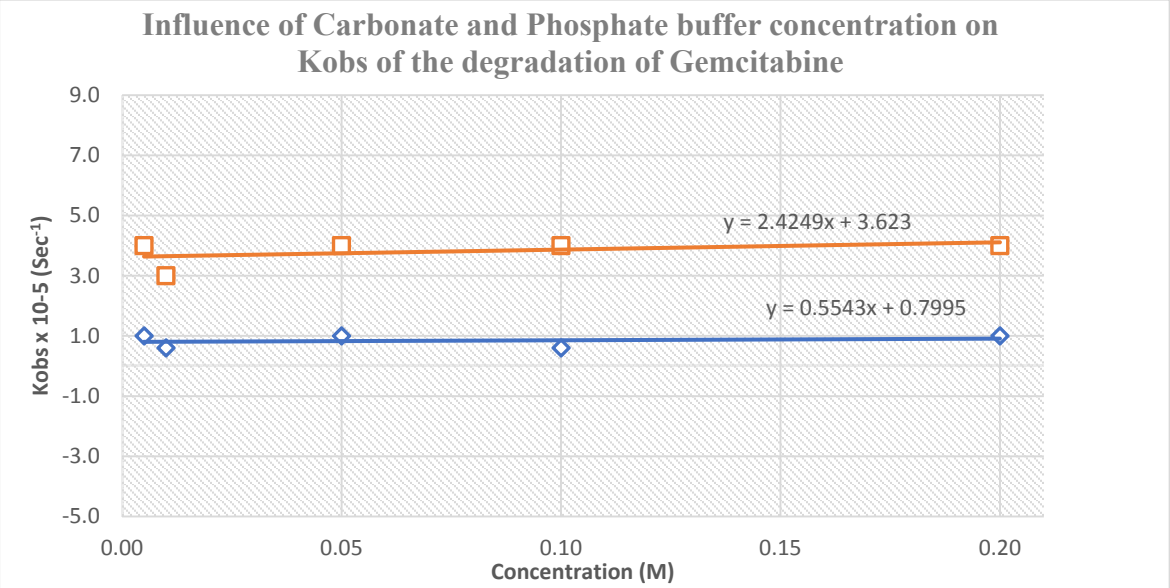

Figure 3: Influence of carbonate concentration at pH 11.0 and phosphate concentration at pH 11.5 on k_{obs} for the degradation of gemcitabine at 70°C. Parallel curves were observed for both carbonate and phosphate buffers at different concentrations (0.005 M to 2.0 M). The k_{obs} values at pH 11 and 11.5 have been extrapolated to zero buffer concentration to delete the influence of buffer ions, resulting in the corrected k'_{obs} in the pH-rate profile. The corrected k'_{obs} for carbonate buffer has a y intercept at 0.7995 and for phosphate buffer has a y intercept at 3.623. (♦ represents pH 11.0, carbonate buffer, pKa_2. ❑ represents pH 11.5, phosphate buffer, pKa_3).

After the correction for buffer catalysis was made for the carbonate and phosphate buffers, the k_{H+} and k_{OH-} were calculated as the intercepts on the y-axis from the portion of the pH-rate profile between pH 1–6 and 10–12, respectively (Figure 2). The specific rate constants were calculated with the use of a non-linear least-squares curve fitting program (Table 4).

Table 4: Specific rate constants of the degradation of gemcitabine at 70°C	
k_{H^+}	$2.22 \times 10^{-5}\ s^{-1}$
k_0	$8.90 \times 10^{-9}\ s^{-1}$
k_{OH^-}	$1.79 \times 10^{-3}\ s^{-1}$

C.4. The Effect of Ionic Strength on the Degradation of Gemcitabine:

The influence of ionic strength on the chemical stability of gemcitabine was investigated at drug concentration of 198 µg/mL with 0.01 M buffer solutions at pH 2.5, 7.0, and 11.0 and 70.0 ± 2°C. The ionic strength was varied between 0.05 and 1.0 M upon addition of various amounts of sodium chloride (Table 5). At both pH 2.5 and 7.0, there was no increase in the rate of degradation upon the increase in ionic strengths. In contrast, the reaction rate increased at pH 11 when the ionic strength was increased from 0.1 M to 1.0 M in carbonate buffer solution (0.01 M), indicating that there is an influence of ionic strength (Figure 4). No influence of ionic strength (µ = 0.05 – 1.0 M) on the chemical stability of gemcitabine injection solution was observed in 0.01 M phosphate buffers at pH 2.5 (pKa_1) and pH 7 (pKa_2). The carbonate buffer (pKa_2) with pH 11 was observed to have an increased rate constant as the ionic strength of the buffer solution increased at > µ= 0.1. This result indicates that a reaction between at least two charged particles does not play an important role in the degradation mechanism of gemcitabine.

Table 5: Influence of Ionic strength on degradation of gemcitabine at different pH buffered solutions.

Ionic Strength (µ)	**pH 2.5 Phosphate Buffer (pKa_1) k_{obs} (s^{-1}) x 10^{-5}**	**pH 7 Phosphate Buffer (pKa_2) k_{obs} (s^{-1}) x 10^{-5}**	**pH 11 Carbonate Buffer (pKa_2) k_{obs} (s^{-1}) x 10^{-5}**
0.05	0.1	0.0006	0.5
0.10	0.1	0.002	0.4
0.30	0.1	0.002	0.5
0.60	0.1	0.001	0.7
1.00	0.09	0.0005	0.8

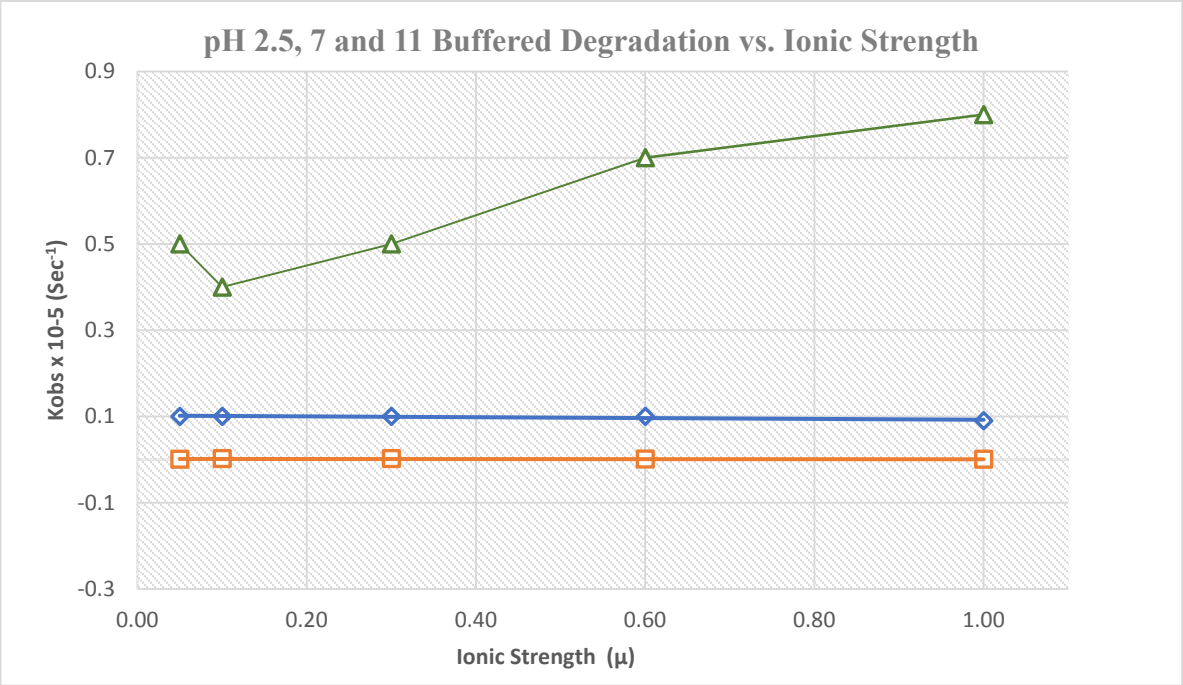

Figure 4: Buffer degradation at different pH vs Ionic Strength Plot: For pH 2.5 & 7.0 buffers, no influence on the rate of degradation observed upon increasing the ionic strength. For pH 11 buffer, rate of reaction linearly increased as the ionic strength (μ = 0.1 – 1.0 M) increased. (♦ represents pH 2.5, phosphate buffer, pKa1. ❑ represents pH 7, phosphate buffer, pKa2. Δ represents pH 11, Carbonate Buffer, pKa2).

Ugye *et al.* observed a linear dependence behavior on the effect of ionic strength on the rate constant of the reaction between formaldehyde and plasma albumin in water solution at neutral pH 7.0 and 37°C [27]. Pablo Valenzuela *et al.* had studied the effects of ionic strength of carbonate buffer at pH 11.1 on the kinetics of the acetylated-δ-chymotrypsin that catalyzes the hydrolysis of N-acetyl-L-tryptophan methyl ester. They observed a linear increase in the rate constants during the increase in ionic strength from μ = 0.1 to 0.5; however, further increase of the ionic strength to μ = 1.0 decreases the rate constant (Table 4) [28]. As a result, it can be predicted for gemcitabine in carbonate buffer at pH 11 (pKa_3) that the increase in ionic strength produced will increase the rate of degradation.

C.5. The Role of Drug Concentration on Degradation:

The effect of sample concentrations on gemcitabine degradation was evaluated at various pH values at 70°C (Table 6 and Figure 5). Sample concentrations were varied from 198 to 1520 µg mL^{-1}, and degradation studies were conducted at pH 2.5, 7.0, and 11.0. The results showed no change in k_{obs} at different drug concentration at pH 2.5 and 7.0 with phosphate buffer. In carbonate buffer at pH 11.0, there was no change in rate constants from 198 to 1140 µg mL^{-1}; however, there was a decrease in k_{obs} at a concentration of 1520 µg mL^{-1}. In summary, only at a high drug concentration (1520 µg mL^{-1}) at pH 11.0, the rate of drug degradation is slower, it may be due to a possible sample precipitation.

Table 6: Rate constant of different buffers in different sample concentrations

Sample Concentration (µg mL^{-1})	**(pH 2.5) Rate Constant k_{obs} (s^{-1}) × 10^{-5}**	**(pH 7) Rate Constant k_{obs} (s^{1}) × 10^{-7}**	**(pH 11) Rate Constant k_{obs} (s^{-1}) × 10^{-5}**
198	**0.1**	0.2	0.5
380	**0.1**	0.02	0.5
760	**0.1**	0.09	0.5
1140	**0.1**	0.03	0.5
1520	**0.1**	0.03	0.4

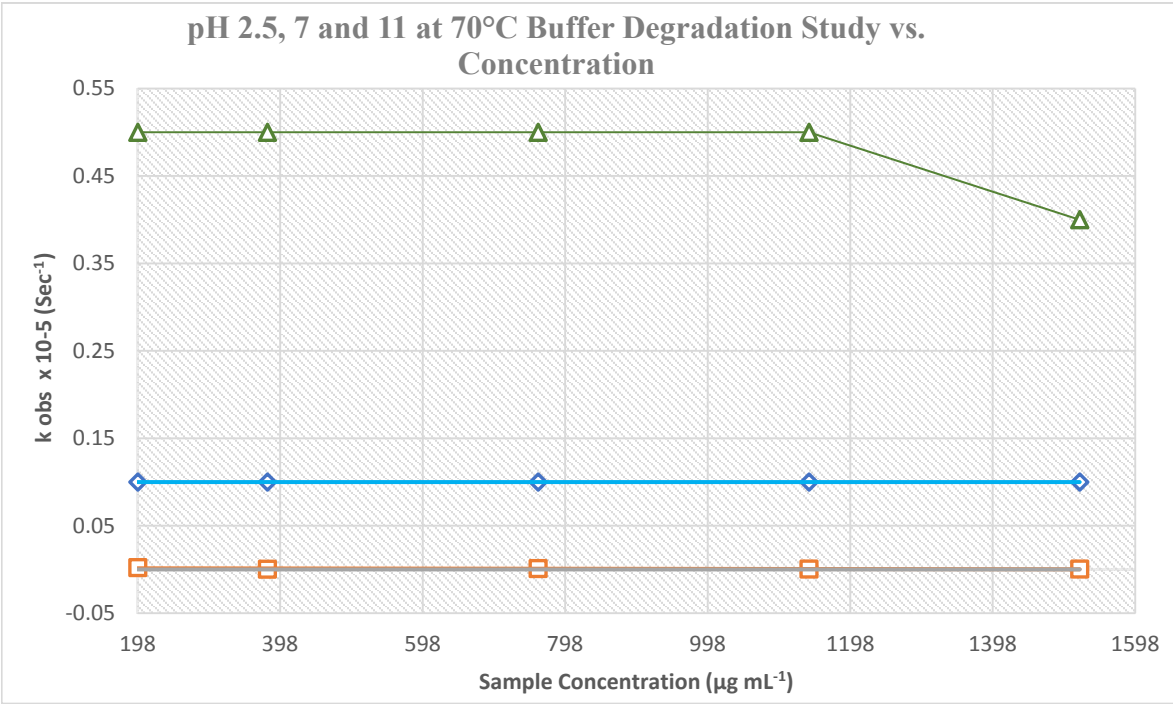

Figure 5: Plot of rate constant vs. sample concentration with different buffers at 70°C. For pH 2.5 and 7.0 buffers, no influence on the rate of degradation was observed upon increasing the sample concentrations. For pH 11 buffer, there was no change in rate constant except at sample concentration 1520 µg mL^{-1}, which falls from level plot. (♦ represents pH 2.5, phosphate buffer, pKa_1. ❑ represents pH 7, phosphate buffer, pKa_2. Δ represents pH 11, carbonate buffer, pKa_2).

C.6. Temperature Effects on the Degradation Reaction:

The impact of temperature on drug degradation at pH 2.5, 7.0, and 11.0 was studied. The Arrhenius equation was used to describe the effects of temperature on three different parts of the pH-rate profile;

$$\ln k_{obs}(T) = \ln A - E_A/R \times 1/T \qquad \text{(Eq. 2)}$$

where A is the frequency factor, E_A is the activation energy, R is the gas constant (8.314 J mol^{-1} K^{-1}), and T is the temperature (K). The degradation rate constants of gemcitabine were derived

from the concentration data obtained on the thermally stressed solutions at four different temperatures at pH 2.5 and three temperatures at pH 7 and pH 11. Table 7 shows the time vs. natural log of concentrations of gemcitabine at pH 2.5 and various temperatures, and these data were used to generate the pseudo first-order degradation plots (Figure 6).

Table 7: Time vs. assay results of gemcitabine Injection Solution of pH 2.5 (phosphate buffer, pKa_1) at 42°C, 60°C, 70°C, and 80°C

Time (day)	ln A (A = % w/w Assay Result) at 42°C	ln A (A = % w/w Assay Result) at 60°C	ln A (A = % w/w Assay Result) at 70°C	ln A (A = % w/w Assay Result) at 80°C
0	4.6 (99.7 %)	4.6 (103.3 %)	4.6 (95 %)	4.6 (95.5 %)
2	---	---	---	4.2 (64.2 %)
4	---	4.4 (83.9 %)	4.3 (74.5 %)	---
5	---	---	---	3.5 (33.7 %)
6	4.6 (96.5 %)	---	---	
7	---	---	---	3.1 (22 %)
9	---	4.3 (70.2 %)	3.9 (48 %)	2.6 (14 %)
10	4.6 (95.6 %)	---	---	---
12	---	---	3.6 (36.5 %)	2.0 (7.3 %)
15	---	4.1 (59.1 %)	---	---
16	4.5 (93 %)		3.2 (24.6 %)	---
19	---	3.9 (51.7 %)	---	---
20	---	---	2.8 (16.5 %)	---
21	4.5 (89.5 %)	---	---	---
22	---	3.9 (47.5 %)	---	---
34	4.4 (82.3 %)	---	---	---
Rate Constant, k (day^{-1})	**0.0056**	**0.0342**	**0.0887**	**0.2151**
R^2	**0.9836**	**0.9904**	**0.9944**	**0.9997**
Order of Reaction	**Pseudo First-Order**	**Pseudo First-Order**	**Pseudo First-Order**	**Pseudo First-Order**

The influence of different temperatures on the degradation of gemcitabine at pH 2.5, 7.0, and 11.0 was studied. Arrhenius plots were constructed to determine their respective activation energies. The linearity of the plot of (k_T) vs. 1/T indicates that the degradation of gemcitabine does follow the Arrhenius equation (Figures 6 and 7). The calculated parameters were extracted from the Arrhenius plot and are shown in Table 8. The activation energy at pH 2.5, 7.0, and 11.0 assumed to show different reaction mechanisms of the proton, solvent, and hydroxyl ion-catalyzed degradation reaction, respectively (Table 8).

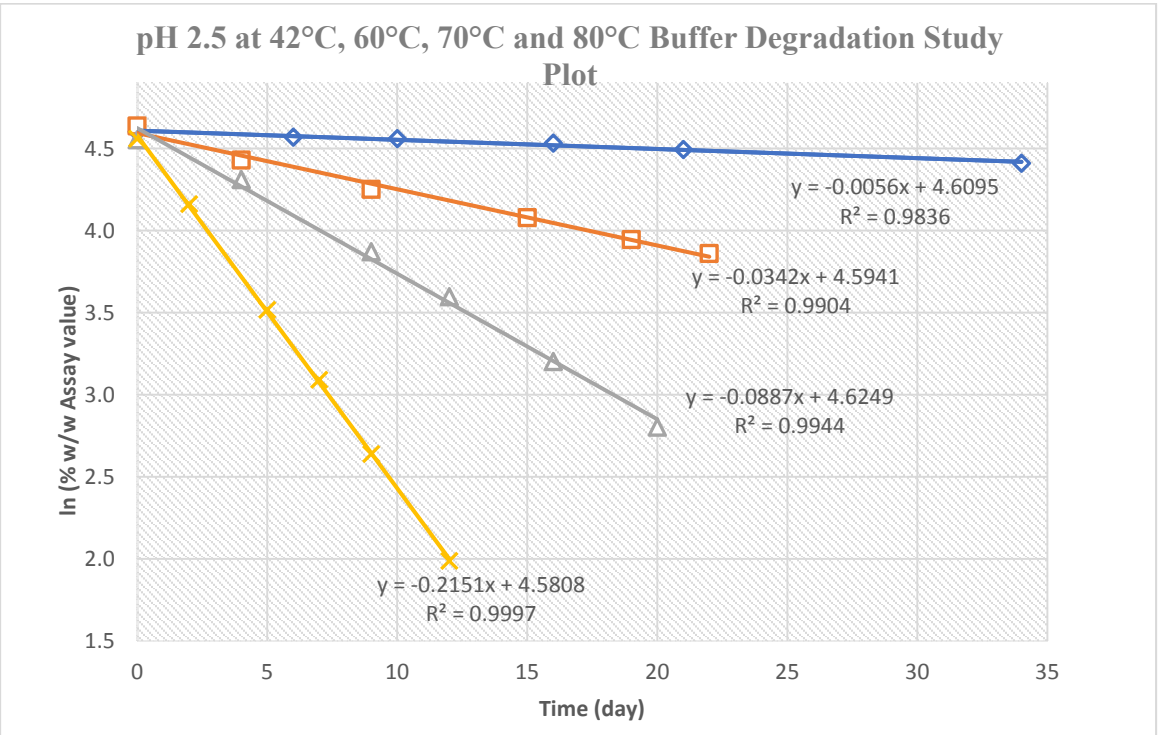

Figure 6: Pseudo first-order plots of the degradation of gemcitabine at the four different temperatures in phosphate buffer (pH 2.5) at various temperatures. (♦, 42°C; ❑, 60°C, Δ, 70°C; and x, 80°C).

(A)

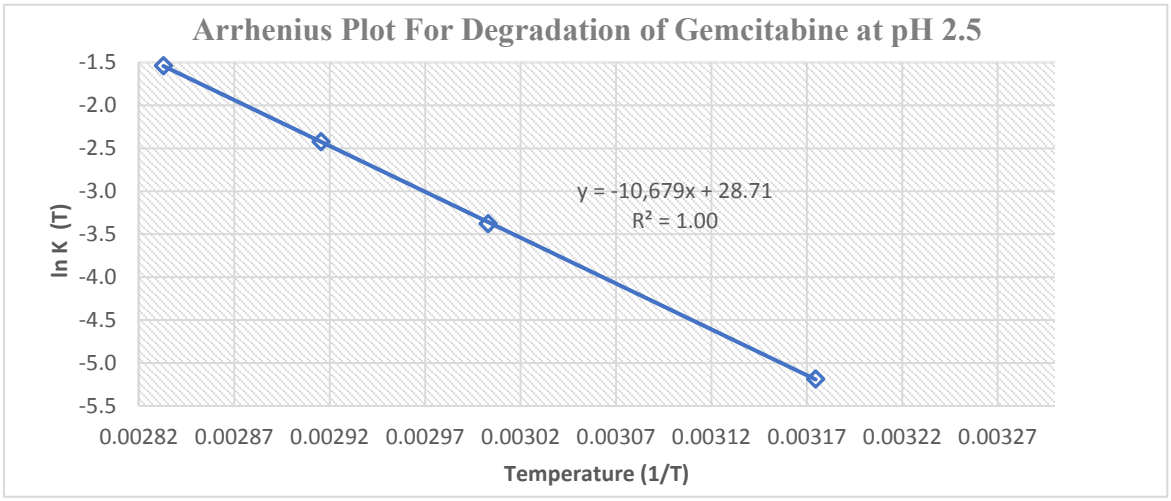

(B)

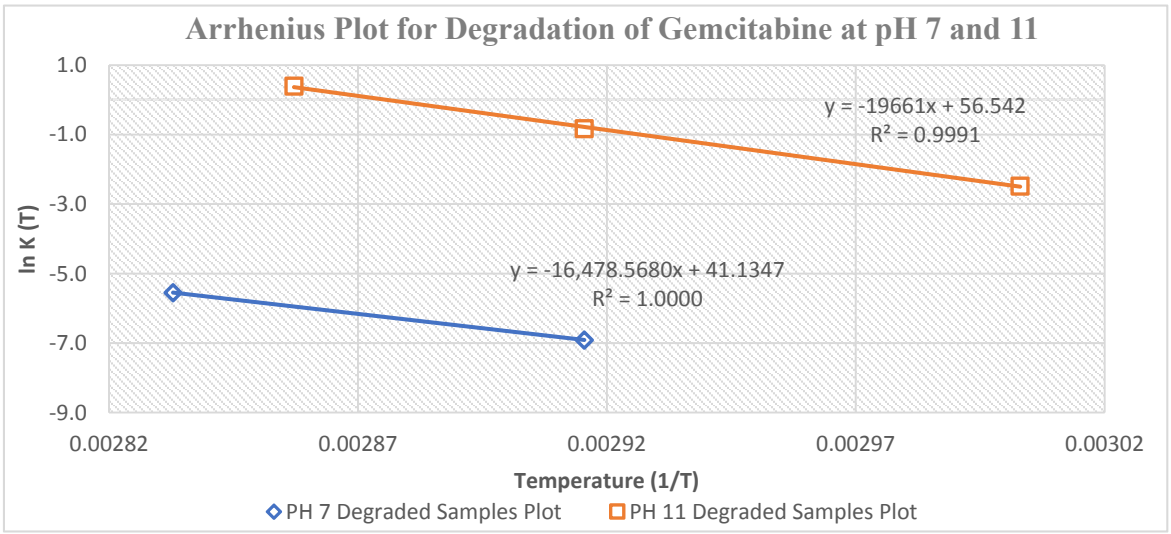

Figure 7. Arrhenius plot for the degradation of gemcitabine at pH **(A)** 2.5 and **(B)** 7.0 and 11.0. Two rate constants of pH 7 at 70°C and 80°C have been selected for best fit of the curve.

Table 8: Parameters from the Arrhenius equation			
pH	**A (day^{-1})**	**E_A ($J\ mol^{-1}$)**	**R^2**
2.5	2.94×10^{12}	8.88×10^{4}	1.0000
7	7.32×10^{17}	1.37×10^{5}	1.0000
11	3.6×10^{24}	1.63×10^{5}	0.9991

The activation energy at pH 2.5 is lower than those at pH 7 and 11 (Table 8) and this difference is possibly due to the difference in degradation mechanism at pH 2.5 compared to that at pH 7 and 11. The degradation at pH 2.5 may involve proton catalysis, while at pH 7 and 11 the degradation mechanisms may involve solvent and/or hydroxyl ion, respectively. At 80°C and pH 7, only 5% gemcitabine was converted into the degradation product while 80% of gemcitabine was converted to the degradation product at pH 11. It is expected that gemcitabine is more stable in mild conditions (pH 7) than the relatively harsh conditions at pH 11. It is interesting to find that the degradation products of gemcitabine at both pH 7.0 and 11 are the same. Although the activation energies at pH 7 and 11 are similar (Table 8), the amount of degradant at pH 7 is lower than at 11; this is presumably due to the difference in degradation mechanisms and the rates of degradation.

C.7. Shelf Life ($t_{95\%}$) of GM Injection Solution at pH 2.5 at 5°C and 25°C:

The Arrhenius plot can be used to calculate degradation rate constants at 25°C and 5°C for pH 2.5 (Figure 7) followed by calculation of the shelf life of gemcitabine ($t_{95\%}$) at these temperatures (Table 9). The calculated shelf-lives for gemcitabine ($t_{95\%}$) are 64 days incubated at 25°C and 2.3 years at 5°C. This result suggests that the injection solution of gemcitabine would be feasible for use in the clinic from the standpoint of chemical stability if it is stored under refrigeration.

Table 9: Gemcitabine Injection Solution $t_{95\%}$ at 5°C and 25°C

A (day^{-1})	E_A /R ($J\ mol^{-1}$)	$t_{95\%}$ at 5°C (year)	$t_{95\%}$ at 25°C (days)
28.71	10679	2.3	64

C.8. Mechanism of Degradation of Gemcitabine:

The degradation of lyophilized form of gemcitabine hydrochloride was previously studied by Anlinker *et al.* [20] and Jansen *et al.* [21]; however, the stability study of gemcitabine injection solution had not been carried out. Thus, this study was done to evaluate the difference in the degradation pathway of an injection solution compared to that of a lyophilized formulation. The degradation study of gemcitabine injection solution was carried out under thermal, acidic, and basic conditions at 70°C for one month, and the degradation products were isolated by HPLC and characterized by NMR and mass spectrometry (MS). In a thermal study at 70°C, the gemcitabine injection solution was degraded up to 94%, and the main degradant product was beta uridine (Scheme 1), which was proposed by Jansen *et al.* [21]. In this current study, a minor product

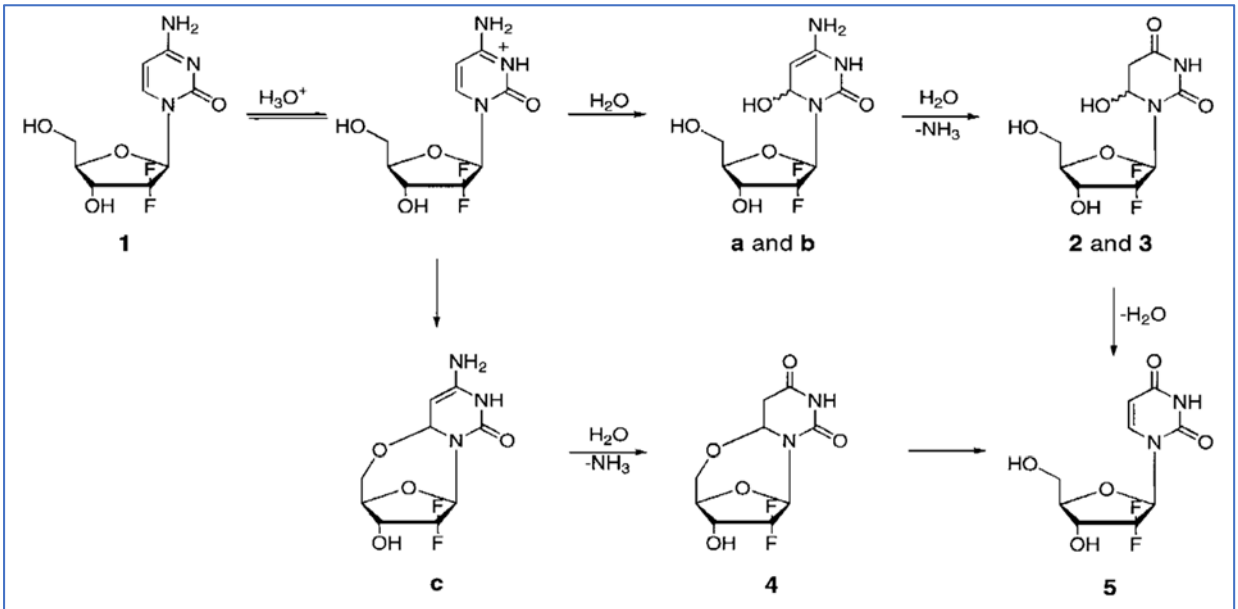

Scheme 1: Proposed deamination pathway of gemcitabine to form β-uridine.
(Reproduced with permission from Elsevier, Permission ID: 4142720182079)

(0.01%) of α-uridine was also observed (Scheme 2). It is noteworthy that 0.4% β-uridine was already formed in gemcitabine injection solution under refrigerated conditions (Figure 8A); however, the heated sample contained 39.58% of β-uridine (Figure 8B).

All of the different stress conditions (i.e., heat, acid, and base) produced β-uridine; however, a lower amount of β-uridine (20.21%) was observed in basic conditions compared to thermal and acidic conditions. In contrast, a higher level of α-uridine was found in basic conditions compared to the acidic conditions (Scheme 2).

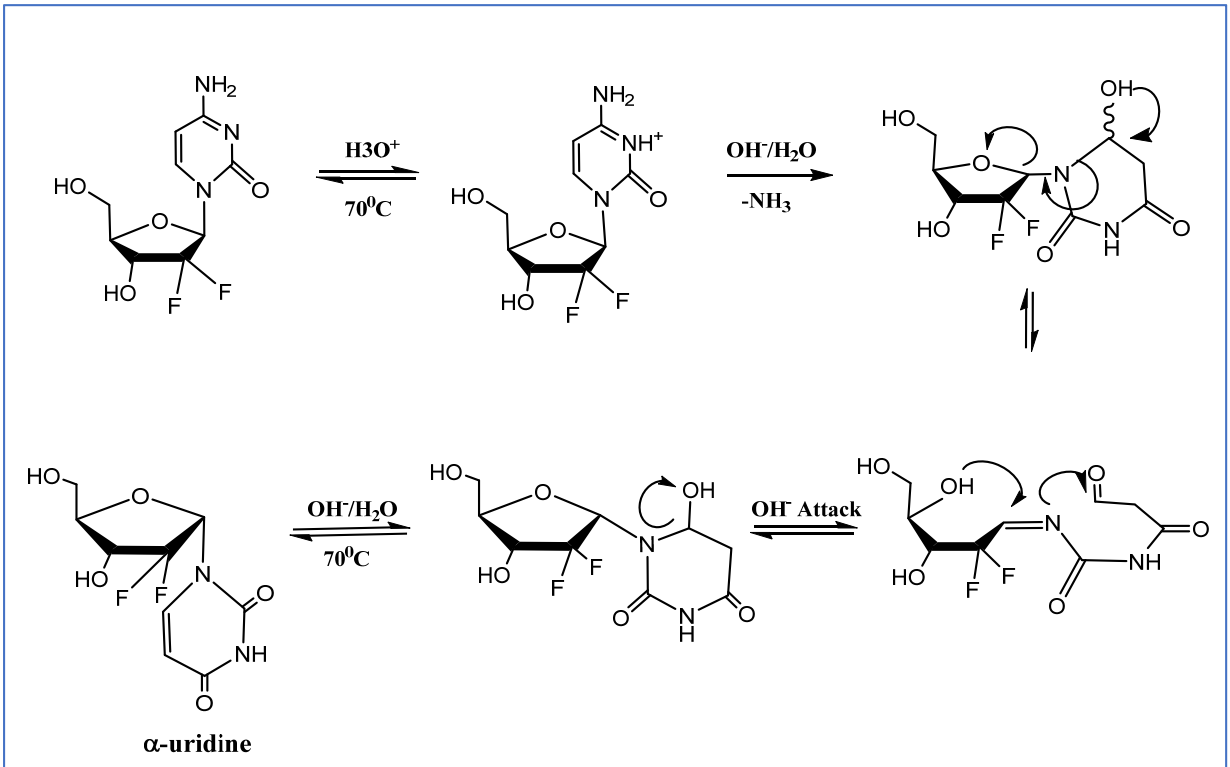

Scheme 2: Proposed deamination pathway of gemcitabine and formation of α- uridine.

A new degradation product, 1-(2-deoxy-2,2-difluoro-α-D-erythro-ribo-pyranosyl)pyrimidine-2,4(1H,3H)-dione, was found under basic conditions at 70°C. This product was isolated using semi-preparative HPLC and characterizd by ^{1}H and ^{13}C NMR and LC/MS/MS. Gemcitabine solution (10 mg/mL) was incubated in acidic solution (1 N HCl) for 4 weeks at 70°C, and 1.5% of gemcitabine remained after 4 weeks as determined by HPLC. The

amount of β-uridine degradation product in the acid conditions was 40.51% compared to 39.58% for the heat-stressed sample of gemcitabine injection solution. This result suggests that the formation of β-uridine was not due to the presence of acid but to heat degradation (Figure 8). The α-uridine was also observed under this thermal acid condition at 70°C, however, it was not observed at 40°C [20]. Both heat and acid-

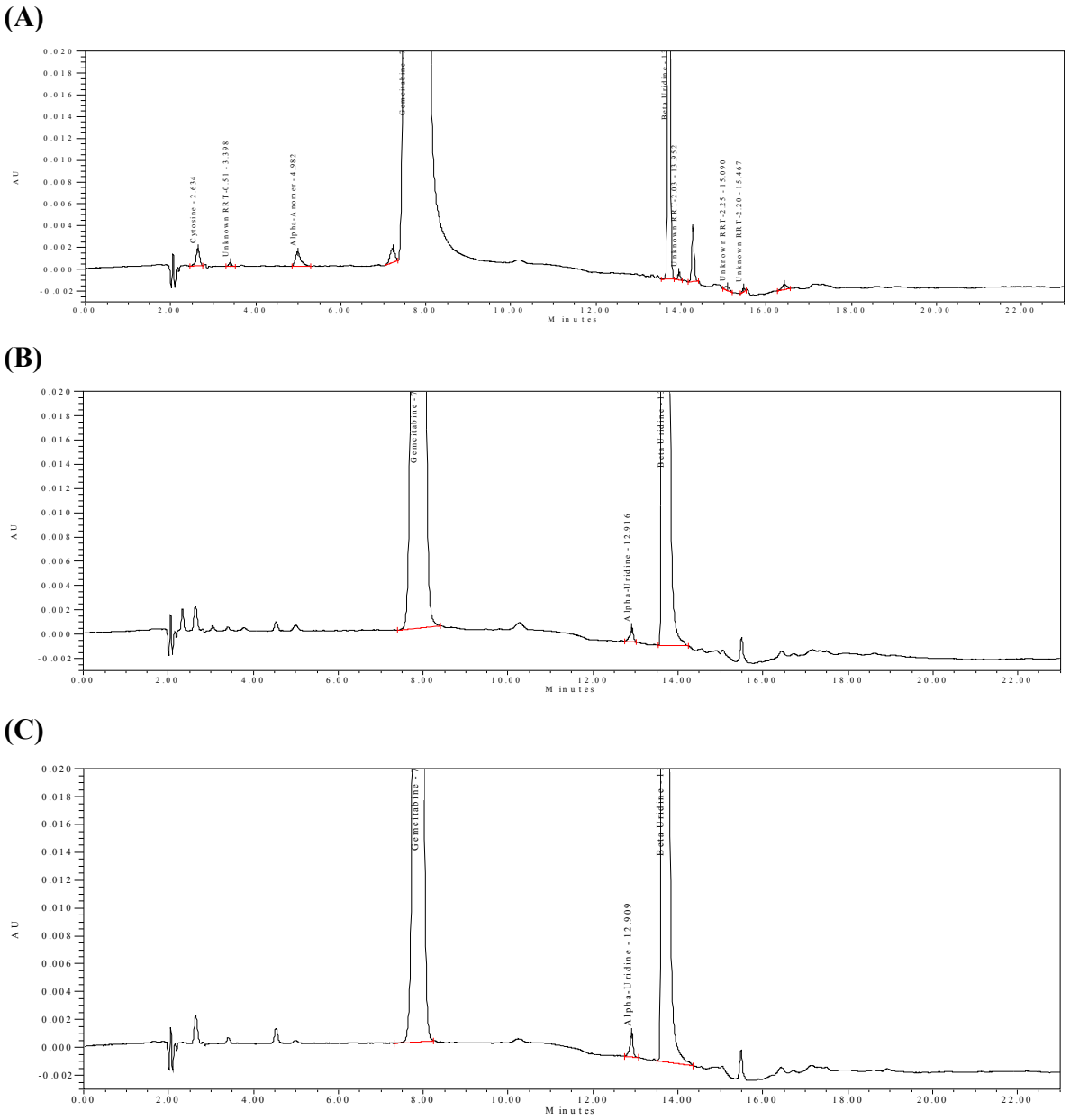

Figure 8: HPLC profiles of 2 mg/mL gemcitabine injection solution after 4 weeks of **(A)** refrigeration, **(B)** incubation at 70°C, and **(C)** incubation in an acid condition at 70°C.

stressed samples at 70°C produced a similar amount of α-uridine (about 0.01%), suggesting that the acid did not influence any further formation of α-uridine. The cytosine base, which elutes at around 2.6 min in the HPLC assay (Figure 8), was not observed as a degradation product under either heat or acidic conditions. Therefore, the cleavage of the cytosine base from the sugar does not occur under heat and acidic

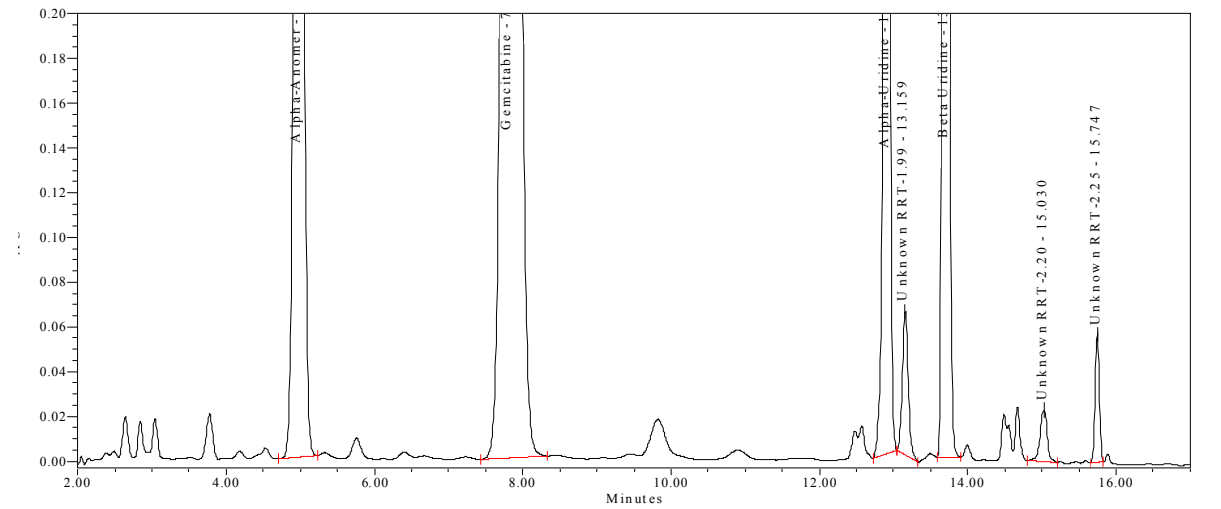

Figure 9: HPLC profiles of 2 mg/mL gemcitabine injection solution after 4 weeks of incubation in a basic solution.

conditions at the elevated temperature of 70°C. This finding is consistent with the work of Nugye and Notari [29], which indicated that un-substituted cytosine nucleosides degrade primarily by heat-independent deamination rather than by cleavage of cytosine from the sugar.

Gemcitabine injection solution (10 mg/mL) was degraded in a basic solution (0.1 N NaOH) for 4 weeks at 70°C (Figure 9). After 4 weeks, 21% of gemcitabine remained in solution. Three degradation products were observed, including α-anomer, α-uridine and β-uridine as were previously isolated and identified by Sally *et al.* [20]. The β-uridine was the heat degradant and was observed in all three stressed conditions, heat, acidic, and basic conditions at 70°C. The β-uridine formation was

due to protonation and deamination by water molecules at 70°C. The α-anomer was formed due to neucleophilic hydroxide attack on the gemcitabine; this formation was unique; forming only under basic-stressed conditions at both 40°C and 70°C (Scheme 3). The formation of an alpha anomer as shown in Scheme 3 had been proposed by Sally *et al*. [20]. The formation of α-uridine was due to protonation and deprotonation of gemcitabine by hydronium ion and hydroxide ion at 70°C. A higher level of α-uridine was observed in basic-stressed solution as compared to heat- and acid stressed sample solutions at 70°C. Therefore, it is evident that α-uridine formation is also sensitive to nucleophilic attack of hydroxide ions.

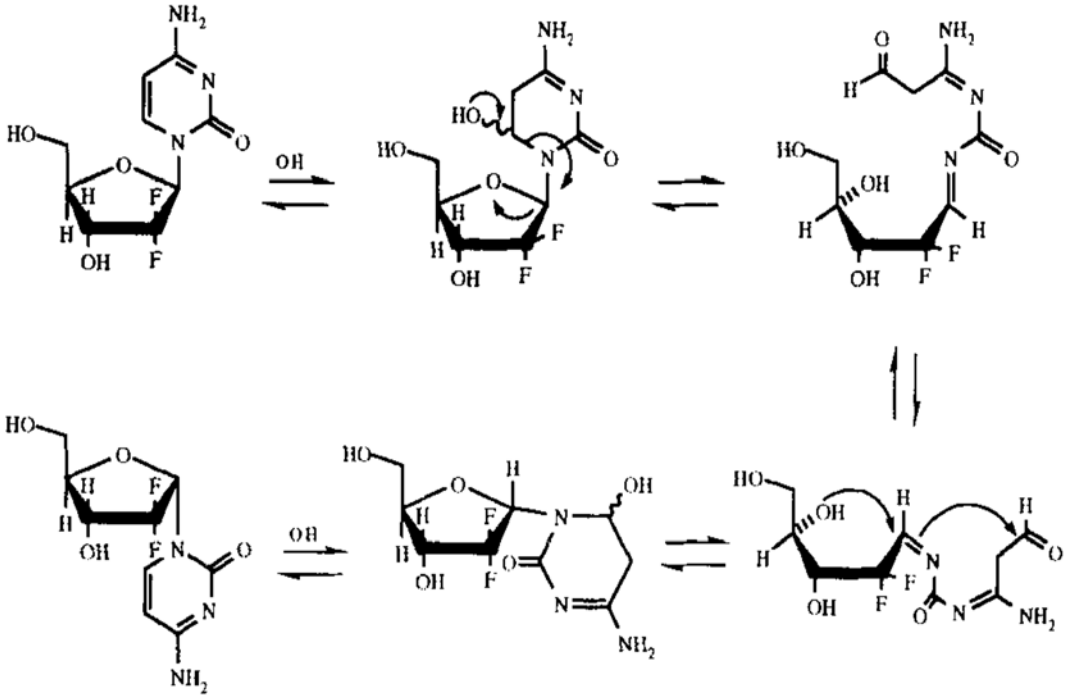

Scheme 3: Proposed deamination pathway of gemcitabine and formation of α-anomer
(Reproduced by permission of Elsevier, Permission ID: 4142721060687).

C.9. Characterization of Degradation Products:

To generate and isolate the degradation products, gemcitabine was incubated in 6 N NaOH at 80°C for 5 h. There were three unknown degradation products that were eluted at 13.16 min, 15.01 min, and 15.75 min at retention times (RT) (Figure 9). Two of those three unknown impurities were not stable under higher thermal basic reaction conditions. The isolated unknown product with RT of 15.01 was confirmed by HPLC-PDA analysis to be a pure component (area = 96%) by the purity angle (0.825), which is less than the purity threshold (1.021) (Figure 10). This isolated impurity was used for further spectroscopic characterization using LC-MS/MS, ^{1}H NMR and ^{13}C NMR.

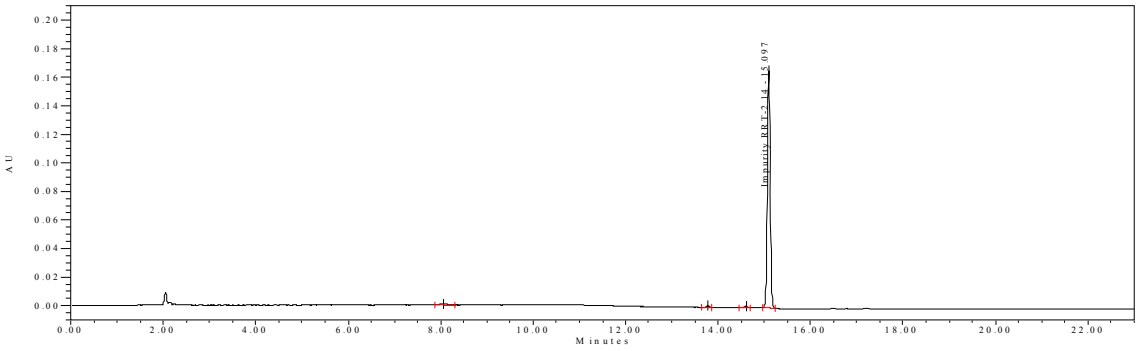

Figure 10: Chromatogram of HPLC-PDA analysis for purity of an unknown degradation product with RT of 15.01.

The degradation of gemcitabine was monitored using UV spectroscopy (Figure 11, Table 10). The UV spectrum of the isolated unknown product with RT of 15.01 was observed at 256 nm (Figure 11A), suggesting that the unknown product has absorbance from a chromophore of cytosine base, which is similar to those from α- and β-uridine. The spectra of mixed known degradation products and unknown

degradation in gemcitabine injection solution are shown in Figure 11B and C, respectively.

(A)

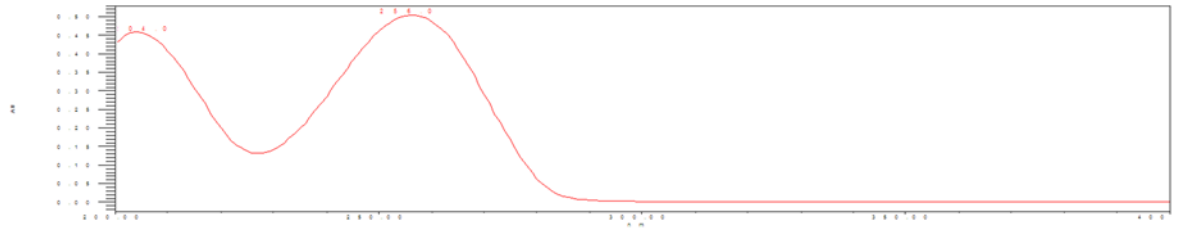

(B)

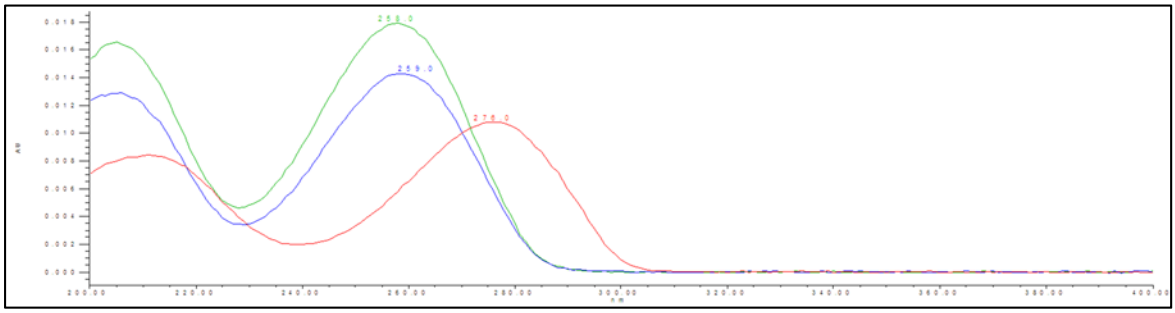

(C)

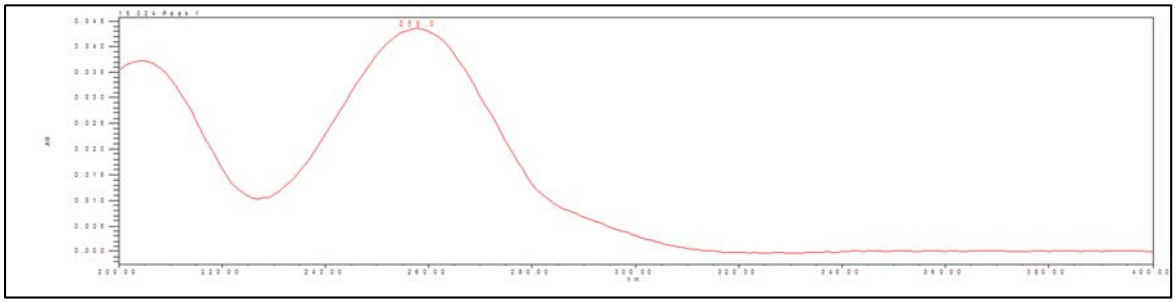

Figure 11: (A) The UV spectrum of an unknown degradation product with a λ_{max} of 256 nm**. (B)** The UV spectra of mixed known impurities. The peak at λ_{max} of 276 nm is for α-anomer (red). The peak at λ_{max} of 259 is for α-uridine (blue). The peak at λ_{max} 258 is for β-uridine (green). **(C)** The UV spectrum of an unknown degradation product of gemcitabine injection solution (2 mg/mL) after 4-weeks incubation in a basic condition at 70°C. The peak at λ_{max} of 258 nm is for an unknown degradation product (red).

Table 10: UV and mass spectra of degradation of known and unknown impurities.		
Degradation Product Name	Retention Time (min)	UV Wavelength (λmax)
α-anomer	4.97	276
α-uridine	12.91	259
β-uridine	14.07	258
Unknown Impurity in the base sample (4 weeks at 70°C)	15.02	258
Unknown Impurity (Isolated)	15.1	256

The isolated unknown compound was also evaluated using mass spectrometry; it has a molecular ion peak at m/z for $[M+H]^+$ at 265. The primary fragment of the parent peak was found at m/z 112 amu, which was from deaminated cytosine base due to the elimination of the ribose group (Figure 12). The deaminated cytosine base (m/z = 112 amu) was also formed as the primary degradation peak and fragmentation pattern for α-uridine (Figure 13 A and B) and β-uridine fragmentation pattern (Figure 13 C and D). On the other hand, the primary peak and fragmentation pattern for α-anomer was cytosine base (m/z = 111 amu) (Figure 13 E and F). Therefore, the unknown impurity contains the same m/z mass spectrum and has a fragmentation pattern similar to that of α- and β-urdine. Because the formation of α-urdine is more favorable than that of β-uridine under basic condition, it is proposed that the unknown product contains a cytosine-deaminated base at the α position. Based on the m/z fragmentation pattern, a reaction pathway for forming the isolated unknown product is shown in Scheme 4.

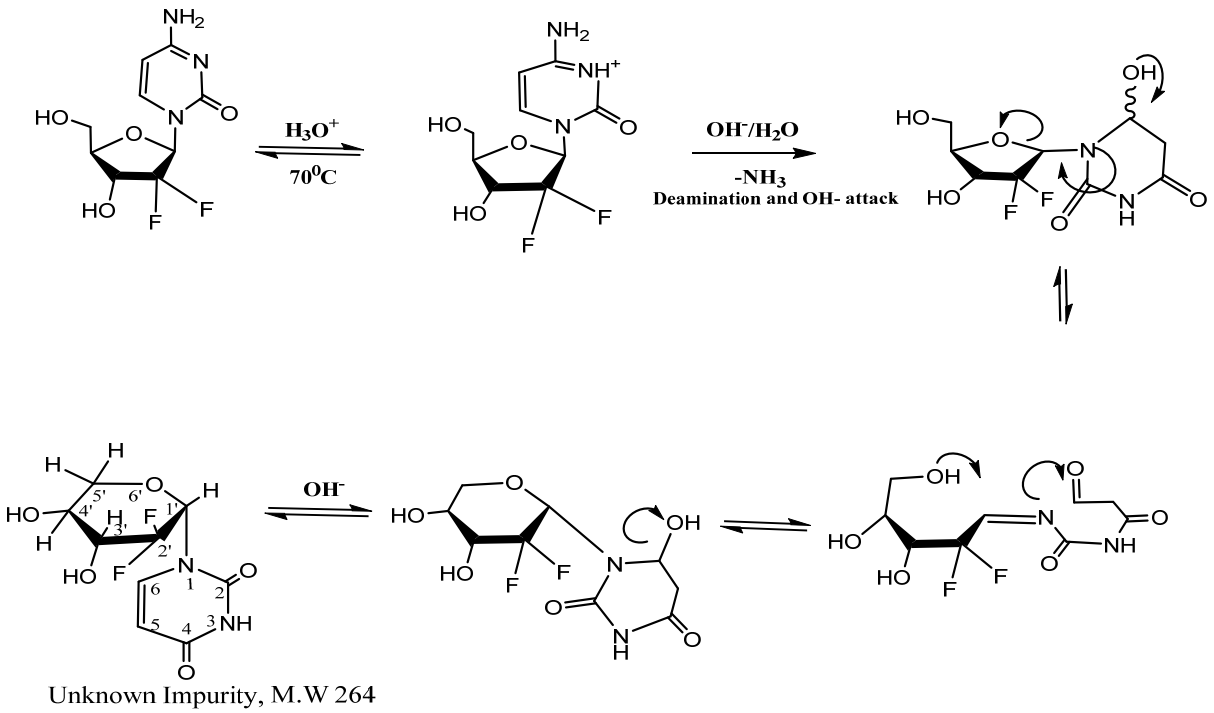

Unknown Impurity, M.W 264

Scheme 4: A proposed pathway for the formation of ribose ring formation in the unknown degradation product.

(A)

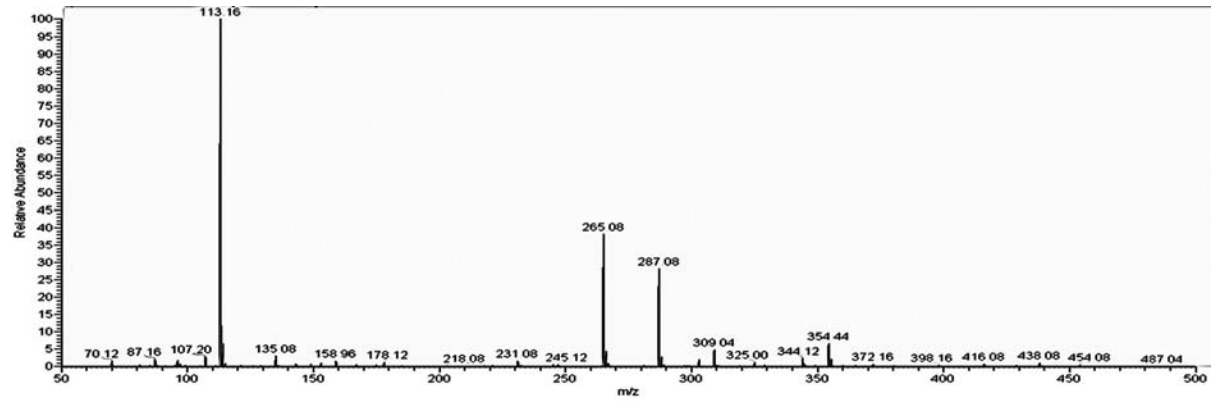

(B)

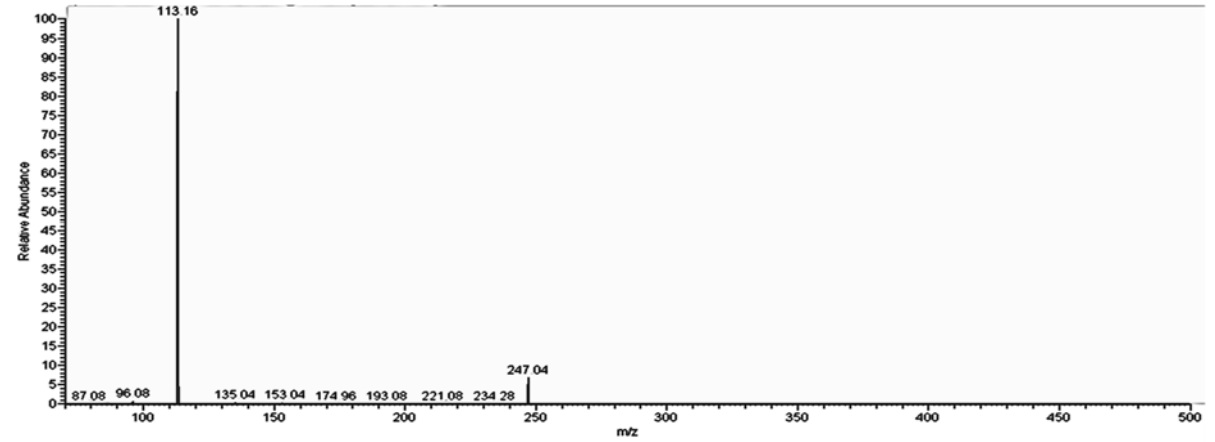

Figure 12: The mass spectrometry spectrum of the isolated unknown degradation product analyzed using **(A)** LC-MS ($[M+H]^+ = 265$) and **(B)** MS/MS mass fragmentation (113.16).

.

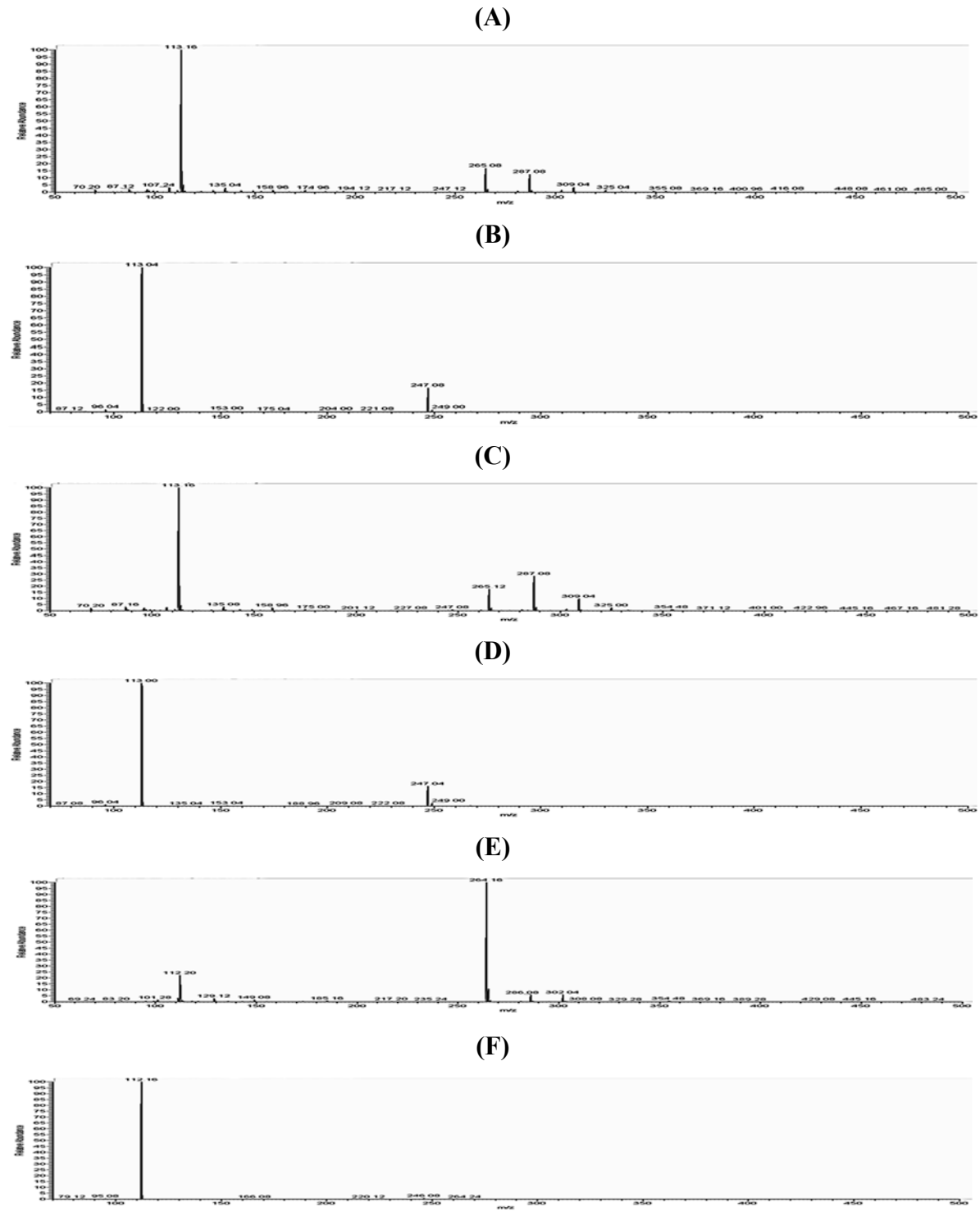

Figure 13: The respective LC-MS and MS/MS mass fragmentation spectra of **(A and B)** α-uridine; (**C and D**) β-uridine; and **(E and F)** α-anomer.

The ^{1}H and ^{13}C chemical shifts from the NMR spectra of various compounds are listed in Table 11. The ^{1}H-NMR of β-uridine has two multiplets at 5.72 ppm and 7.84 ppm [20], respectively, which correspond to the 5 and 6 positions of the cytosine base pyrimidine moiety. In-addition, the signals at 6.13, 4.27, 3.93, 3.77, and 3.88 ppm correspond to the 1′, 3′, 4′, 5′, and 5′ protons, respectively. The corresponding ^{13}C NMR signals for positions 5, 6, 1′, 3′, 4′, and 5′ are at 102.98, 141.88, 85.29, 70.46, 82.72, and 60.47 ppm, respectively.

Another degradation product of gemcitabine is the α-isoform product II (Table 11), which has structure similar to that of β-uridine for the pyrimidine moiety and ribose base protons [30]. The ^{1}H NMR spectrum of the isolated product has peaks at 5.63 ppm and 7.53 ppm corresponding to the 5 and 6 positions of the cytosine base pyrimidine moiety. The peaks with chemical shifts of 6.13, 4.05, 3.87, and 3.81 ppm are from 1′, 3′, 4′, and 5′ protons, respectively, which have similarities to the α-isomer product II [30] and β-uridine [20] (Table 11). For the cytosine base, the ^{13}C NMR signals at positions 2, 4, 5, and 6 are 150.75, 164.46, 101.66, and 141.67 ppm, respectively; these signals are similar to those in α- or β-uridine. For the sugar moiety, the ^{13}C signals at 114.92, 129.07, 70, 65.45 and 65.67 ppm are from carbons at positions 1′, 2′, 3′, 4′, and 5′, respectively, which are similar to those from α-isomer product II [30] (Table 11). The DEPT-135 NMR data for isolated unknown products are provided in Table 11.

The coupling constant (J) values for the protons located at the 1′ position of the isoform product II [30] and isolated products are 19.61 Hz and 19.97 Hz, respectively (Table 11). The data suggest that there is no change in dihedral angle between the 1′

proton and the adjacent fluorine atoms. Similarly, the coupling constant values for the protons located at position 6 of the isoform product [30] and the isolated product are 2.62 Hz and 2.15 Hz, respectively (Table 11). Based on the above data comparison, the isolated product was identified as 1-(2-deoxy-2,2-difluoro-α-D-erythro-ribopyranosyl)pyrimidin-2,4(1H,3H)-dione (Scheme 4).

Table 11: Comparative NMR assignments for β-uridine, α-Isoform Impurity II and the Unknown Isolated Impurity

Position	β-uridine [20] (Authentic 4*)		α-Isoform Impurity II [30]			Unknown Isolated Impurity		
	^{1}H NMR (ppm)	^{13}C NMR (ppm)	^{1}H NMR (ppm)	^{13}C NMR (ppm)	DEPT-135 (ppm)	^{1}H NMR (ppm)	^{13}C NMR (ppm)	DEPT-135 (ppm)
2	---	151.93	---	160	---	---	150.75	151
4	---	165.62	---	163	---	---	164.46	168.9
5	5.72 (d, 1H)	102.98	6.09 – 6.12 (d, 1H)	95.0	95.1	5.61 – 5.63 (d, 1H)	101.66	102
6	7.84 (dd, 1H)	141.88	7.82 (dd, 1H, JH5,H6=7.95 Hz, JH6,F=2.62 Hz)	144.5	144.4	7.51 – 7.53 (dd, 1H, JH5,H6=8 Hz, JH6,F=2.15 Hz)	141.67	142
1′	6.13 (dd, 1H)	85.29	6.16 – 6.21 (d, 1H, JH1′,F=19.61 Hz)	76.8	76.9	6.03 – 6.08 (d, 1H, JH1′,F=19.97 Hz)	114.92	115
2′	---	123.93	---	118	---	---	129.07	129
3′	4.27 (m, 1H)	70.46	4.12 – 4.16 (m, 1H)	69.8	69.8	4.05 – 4.15 (m, 1H)	70	70
4′	3.93 (m, 1H)	82.72	3.94 – 4.00 (m, 1H)	65.3	65.3	3.87 – 3.95 (m, 1H)	65.45	65.45
5′	3.77 (m, 2H)	60.47	3.85 – 3.92 (m, 2H)	65.8	65.8	3.78 - 3.81 (m, 2H)	65.67	65.67
5′	3.88	---	---	---		---	---	---

---, Not applicable, d-doublet and m-multiplet.

D. CONCLUSIONS

The degradation of gemcitabine injection solution follows pseudo first-order kinetic reactions. The pH-rate profile of gemcitabine shows three distinctive regions that are catalyzed by protons, solvent, and hydroxide ion; however, there might be something more than specific proton and hydroxyl catalysis are likely going on. Gemcitabine molecule was more stable in the solvent region of pH range 7–9.5 than in lower and higher pH regions. The stability of gemcitabine injection solution was determined at pH 2.5 and various temperatures for obtaining the Arrhenius plot. At pH 2.5, gemcitabine injection solution has a shelf-life of two years in refrigerated conditions and only two months at room temperature. It is suggested that gemcitabine injection solution can be developed for refrigerated formulation.

In neutral and alkaline solution, gemcitabine showed similar degradation products, but presumably through different mechanisms. At neutral pH, the regularly observed degradation products were accompanied by another degradation product. Thermal degradation of gemcitabine at 70°C for 4 weeks produced α- (0.01%) and β-uridine (40%), in which water molecules act as acid and base. In contrast. the degradation of gemcitabine in acidic media (1 N HCl) at 70°C for 4 weeks did not show any anomerization, which is consistent with the finding by Sally *et al.* [20] in the 40°C degradation study. It is concluded that the formation of β-uridine (40%) is due only to the thermal stress condition at 30°C, 40°C and 70°C.

Anomerization products such as α-anomer (17%) of gemcitabine and α-uridine (8%) are formed under basic-stressed conditions (0.1 N NaOH) at 70°C. Although β-uridine (~ 20 %) is observed under this condition, it is at a lower level than in thermal- or acid-stressed conditions at 70°C. The higher level of α-uridine formation in basic-stressed solution at 70°C was due to nucleophilic attack by the hydroxide ion and/or water molecules. Finally, this study elucidated

one significant degradation product under basic conditions as 1-(2-deoxy-2,2-difluoro-α-D-erythro-ribopyranosyl)pyrimidin-2,4(1H,3H)-dione.

E. REFERENCES

1. Gemcitabine–A review of its pharmacology and clinical potential in non-small cell lung cancer and pancreatic cancer. Noble S and Goa K., Drugs, 1997, 54 (3); 447-472.
2. Comparison of the cellular pharmacokinetics and toxicity of 2',2'-difluorodeoxycytidine and 1-beta-D-arabinofuranosylcytosine. Heinemann, V.; Hertel, L. W., Grindey G. B. and Plunkett W., Cancer Res. 1988, 48 (14), 4024-4031.
3. Synthesis Synthesis of 2-deoxy-2,2-difluoro-D-ribose and 2-deoxy-2,2'-difluoro-D-ribofuranosyl nucleosides. L. W. Hertel, S. J. Kroin, J. W. Misner and J. M. Tustin, J. Org. Chem., 1988, 53 (11), 2406-2409.
4. Antiviral activity spectrum and target of action of different classes of nucleosides Analogues. De Clercq, E., Nucleosides & Nucleotides. 1994, Vol 13 (687), pp 1271-1295.
5. Gemcitabine: a cytidine analogue active against solid tumors, Hui, Y.F. and Reitz, J., Am. J. Health Syst. Pharm., 1997, 54 (2), 162-170.
6. New chemotherapeutic agents prolong survival and improve quality of life in non-small cell lung cancer: a review of the literature and future directions. Bunn, P.A., and Kelly K., Clinical Cancer Res., 1998, 4 (5), 1087-1100.
7. Efficacy and safety profile of gemcitabine in non-small-cell lung cancer: a phase II study. Abratt, R.P., Bezwoda, W.R., Falkson, G., Goedhals, L., Hacking. D. and Rugg TA., J. Clin. Oncol., 1994, 12 (8), 1535 – 1540.
8. Nucleic acids. VI. The mechanism of the deamination of cytidine. W. J. Wechter and R. C. Kelly, Coll.Czechoslovak Chem. Commun, 1970, 35 (7), 1991-2002.

9. Comparative kinetics of cytosine nucleosides. Influence of a 6-methyl substituent on degradation rates and pathways in aqueous buffers. Notari, R. E.; Witiak, D. T., De Young J. L and Lin A. J., J. Med. Chem. 1972, 15 (12), 1207-1214.

10. Nucleic acid hydrolysis. I. Isomerization and anomerization of pyrimidic deoxyribonucleosides in an acidic medium. Cadet J. and Teoule, R., J. Am. Chem. Soc. 1974, 96 (20), 6517-6519.

11. Rapid determination of Gemcitabine and its metabolite in human plasma by LC-MS/MS through micro protein precipitation with minimum matrix effect. Ling-Zhi Wang, Wei-Peng Young, Ross-A. Soo, Soo-Chin Lee, Richie Soong, How-Sung Lee and Boon-Cher Goh, J. Pharm. Sci. Res., 2009, 1 (3), 23-32.

12. The base catalysed anomerisation of β-5-formyluridine; crystal and molecular structure of α-5-formyluridine. V. W. Armstrong, J. K. Dattagupat, F. Eckstein and W. Saenger, Nucleic Acid Res. 1976, 3 (7)), 1791-1810.

13. Stability-indication HPLC determination of Gemcitabine in pharmaceutical formulations. Rahul Singh, Ashok K. Shakya, Rajashri Naik and Naeem Shalan, Int. J. Analy. Chem., 2015, 2015 (2015), Hindawi, Article ID: 862592, 1-12.

14. Method validation of an LC-MS/MS method for the determination of Gemcitabine and 2'-deoxy-2',2'-difluorouridine (Di-du) in etrahydrouridine (THU)-treated human plasma. Elizabeth M. Peterson, Erica Nachi, Brandon Retke, Corey Ohnmacht and Curtis Sheldon, Celerion (www.celerion.com), Applied Translational Medicine, White Paper, 1-4.

15. Method development and validation for the assay of Gemcitabine hydrochloride in pharmaceutical dosage forms by RP-HPLC. R. Murali Krishna, M. Ramesh, M. Buela and T. Siva Kumar, Indo Am. J. Pharm. Res., 2011, 1 (3); 189-195.

16. A stability indication UPLC method for the rapid separation of related components of Gemcitabine hydrochloride. Ch. Surya Naga Malleswararao, M. V. Suryanaryana, K. Krishana and K. Mukkanti, J. Liq. Chrom. & Rel. Tech., 2012, 35 (18), 2511-2523.

17. Simultaneous determination of Gemcitabine di- and triphosphate in human blood mononuclear and cancer cells by RP-HPLC and UV detection. R. Losa, Sierra MI, Gion MO, Esteban E and Buesa JM., J. of Chrom. B., 2006, 840 (1), 44-49.

18. A stability-indicating RP-HPLC method for the estimation of Gemcitabine hydrochloride in injectable dosage forms. Shaik Mastanamma, G. Ramkumar, D. Anantha Kumar and J. V. L. N. Seshagiri Rao, E-J. Chem., 2010, 7 (S1), S239 -S244.

19. To determine the half-life for gemcitabine hydrochloride using microcalorimetry. Liu Dai-Huo, Wei-Wei Zhao and Zhong-Xiao Li, J. Therm. Analy. Calorim., 2014, 115 (2), 1793-1797.

20. Degradation chemistry of gemcitabine hydrochloride, a new antitumor agent. Sally L. Anliker, Michael S McClure, Thomas C. Britton, Erwin A Stephan, Steven R. Maple and Gary G. Cooke, J. Pharm. Sci., 1994, 83 (5), 716-719.

21. The degradation of the antitumor agent gemcitaibne hydrochloride in an acidic aqueous solution at pH 3.2 and identification of degradation products. Patrick J. Jansen, Michael J. Akers, Robert M. Amos, Steven W Baertschi, Gary G. Cooke, Douglas E. Dorman, Craig A. J. Kemp, Steven R. Maple and Karen A. Mccune, J. Pharm. Sci., 2000, 89 (7), 885-891.

22. Gemcitabine Hydrochloride Assay and Impurities Method, United States Pharmacopeia, USP 39-NF 34, USA Edition, 2016, 4098.

23. Kinetics of iodination: effect of solvent on hydroxyl ionization and iodination of l-tyrosine and 3-iodo-l-tyrosine. W. E. Mayberry and Thomas J. Hockert, The J. of Biological Chemistry, 1970, 245 (4), 697 – 700.

24. A systematics study on the chemical stability of ifosfamide. G.P. Kaijser, J. H. Beijnen, A. Bult, M. H. Hogeboom and W. J. M. Underberg, J. Pharm. & Biomed. Analysis, 1991, 9 (10 – 12), 1061 – 1067.

25. Kinetic landscape of a peptide bond-forming prolyl oligopeptidase. Clarissa M. Czekster and James H. Naismith, Biochemistry, 2017, 56 (15), 2086-2095.

26. Ready to be infused gemcitabine solution (Section: 0042); Patent # EP2656848B1, Publication Date: 8 Apr. 2015, Application# EP20130165862.

27. The Effect of pH and ionic strength on rate of reaction of plasma albumin with formaldehyde in water solution and ethanol-water binary mixtures. Ugye T. J., Uzairu A., Idris S. O. and Kwanashie H. O., Int. J. Res. Chem.Environ., 2013, 3 (4), 8-12.

28. Alkaline pH dependence of δ-chymotrypsin-catalyzed hydrolysis of specific substrates. Pablo Valenzuela and Myron L. Bender, Proc Natl. Acad. Sci., 1969, 63 (4), 1214 – 1221.

29. Substituent effects on degradation rates and pathways of cytosine nucleosides. Nguyen N. A. and Notari R. E., J. Pharm. Sci. 1989, 78 (10), 802-806.

30. Separation, isolation, and characterization of isoform impurities of gemcitabine formed during the anomerization of protected α-gemcitabine to gemcitabine. S.G. Hiriyanna, K. Bashavaia, Hari N. Pati and Bijay K. Mishra, J. Liq. Chrom. & Rel. Tech., 2007, 30 (20), 3093-3105.